Ph.D. Thesis

Fabrication of Modified Poly(ethylene oxide) Hydrogel Films for Biomedical Applications Using E-Beam

Graduate School of Yeungnam University

Department of Advanced Organic Materials Engineering

Major in Advanced Organic Materials Engineering

HARYANTO

Advisor: Professor Seong Cheol Kim

June 2015

Ph.D. Thesis

Fabrication of Modified Poly(ethylene oxide) Hydrogel Films for Biomedical Applications Using E-Beam

Advisor: Professor Seong Cheol Kim

Presented as Ph.D. Thesis

June 2015

Graduate School of Yeungnam University

Department of Advanced Organic Materials Engineering

Major in Advanced Organic Materials Engineering

HARYANTO

Haryanto's Ph.D. Thesis is approved by

Committee member: Prof. Sung Soo Han _____

Committee member: Prof. Seong Cheol Kim _____

Committee member: Prof. Se Hyun Kim _____

Committee member: Prof. Jong Oh Kim _____

Committee member: Prof. PilHo Huh _____

June 2015

Graduate School of Yeungnam University

ACKNOWLEDGEMENTS

I would like to thank my advisor, Prof. Seong Cheol Kim for his never-ending support, patience and kindness throughout this study. His experience and future vision about polymer applications has encouraged me to explore more about polymer especially for medical applications.

I wish to thank my wife Sunarni for her loves, patience and endless supports and also my sincere thanks to my beloved daughters (Ifah, Fitri, Nabila and Hana) who always support me through their prayers and endorse me to graduate earlier. My personal gratitude goes to my father Alm H. Achmari, my mother Hj. Suparti and my sisters (Alm Sri rahayu, Indah Purwati and Suhartini) for their attentions and prays throughout my life.

Special thanks go to Kim Jintae for helping me in all matters. And also many thanks to all International and Indonesian students for generous friendship that makes me comfortable to study in this campus.

Gyeongsan, June 2015

Haryanto

Yeungnam University

ABSTRACT

Recently, synthetic polymer hydrogels have emerged as a promising biomaterial for biomedical applications because of their biocompatibility, water absorption capability, degradability and better mechanical properties than natural polymer hydrogels. Therefore, the current study was undertaken with the main objective of developing modified poly(ethylene oxide) (PEO) hydrogel films with poly(ethylene glycol) diacrylate (PEGDA), poly(ethylene glycol) dicarboxcylate (PEGDC), poly(ethylene glycol) dimethacrylate (PEGDMA) and hyperbranch polyglycidol (HPG) with enhanced properties using electron beam (E-Beam) for three major applications namely wound dressing, anti-adhesion barrier and tissue engineering scaffold.

Cross-linked PEGDA/PEO hydrogel was developed for wound dressing application. PEO with different molecular weights and various PEGDA/PEO compositions were irradiated in order to obtain cross-linked hydrogels using e-beam with various beam intensities. The contents of the PEGDA influenced the gel fraction, swelling ratio, mechanical properties, and water vapor transmission rate. Healing under the wet environment of the hydrogel dressing was faster than with a gauze control and a commercial reference. The results demonstrate the possibility of the facile production of mechanically robust and transparent wound dressing materials with improved wound healing characteristics.

The cross-linked PEGDC/PEO and PEGDMA/PEO hydrogels were developed for an anti-adhesion barrier application. Three different compositions (10% PEGDC, 10% PEGDMA, 5% PEGDC–5% PEGDMA) were used to prepare crosslinked hydrogel films. Among them, 10% PEGDC hydrogel film exhibited the highest tissue adherence. The result also indicated that the carboxyl groups in PEGDC affect the tissue adherence of hydrogel films via H-bonding interactions. In animal studies, 10% PEGDC anti-adhesion hydrogel film demonstrated better anti-adhesive effect compared to Guardix-SG®.

A microporous hydrogel scaffold was developed from HPG and PEO using e-beam induced cross-linking for tissue engineering applications. In this study, HPG was synthesized from glycidol using trimethylol propane as a core initiator and cross-linked hydrogels were made using 0%, 10%, 20% and 30% HPG with respect to PEO. Increasing the HPG content increased the pore size of the hydrogel scaffold, as well as the porosity. The pore size of hydrogel scaffolds could be easily tailored by controlling the content of HPG in the polymer blend. Evaluation of the cytotoxicity demonstrated that HPG/PEO hydrogel can function as a potential material for tissue engineering scaffolds.

This study shows the potential of modified PEO hydrogel films in biomedical applications especially as wound dressing, anti-adhesion barrier and tissue engineering scaffold.

TABLE OF CONTENTS

LIST OF TABLES

LIST OF FIGURES

CHAPTER I

INTRODUCTION AND MOTIVATION

I.1. Review of hydrogel for biomedical applications

Polymer hydrogels are a still new, fast developing group of materials, growing broad application in many fields, especially biomedical materials, pharmacy, medicine and agriculture. One of the most promising class of biomaterials seem to be hydrogels. The word “biomaterial” is generally used to recognize materials for biomedical applications. For over thirty years hydrogels have been used in numerous biomedical applications such as drug delivery, cell carriers, wound dressing, tissue engineering scaffold, contact lenses, anti-adhesion barrier and absorbable sutures as well as in many other areas of clinical practice.

Hydrogels are polymeric networks which have the ability to absorb and hold water from 10–20% (an arbitrary lower limit) up to thousands of times their dry weight within the spaces available among the polymeric chains. As the term network implies, crosslinks have to be present to avoid dissolution of hydrophilic polymer chains/segments into the aqueous phase. Hydrogels may be chemically stable or they may degrade and eventually disintegrate and dissolve [1,2].

The water holding capacity of the hydrogels arise mainly due to the presence of hydrophilic groups, viz. amino, carboxyl and hydroxyl groups, in the polymer chains. Higher the number of the hydrophilic groups, higher is the water

holding capacity while with an increase in the crosslinking density there is a decrease in the equilibrium swelling due to the decrease in the hydrophilic groups. As the crosslinking density increases, there is a subsequent increase in the hydrophobicity and a corresponding decrease in the stretchability of the polymer network. As mentioned above, hydrogels are crosslinked polymeric networks and hence provide the hydrogel with a 3-dimensional polymeric network structure [3].

The term hydrogel describes three-dimensional network structures obtained from a class of synthetic and/or natural polymers which can absorb and retain significant amount of water. They are insoluble due to the presence of chemical (tie-points, junctions) and/or physical crosslinks [4,5].

Hydrogel of many synthetic and natural polymers have been produced with their end use mainly in pharmaceutical and biomedical fields [6]. Due to their high water absorption capacity and biocompatibility they have been used in many medical applications. A list of hydrogels with their applications is shown in Table 1.

Table 1. Biomedical applications of hydrogels

Application	Hydrogel
Wound healing	Polyvinyl alcohol, gelatin, carboxymethyl cellulose, hyaluronan, poly(vinylpyrrolidone), polyethylene glycol.
Cosmetic, pharmaceutical.	xanthan, pectin, carrageenan, alginate, chitosan.
Tissue	Agaraose, poly(vinyl alcohol), poly(acrylic acid),

Engineering.	hyaluronan, collagen.
Drug carrier	Polyvinyl alcohol, carboxymethyl cellulose.
Contact lenses	Silicone hydrogel, PVA, Hema.
Anti-adhesion barrier	CMC, hyaluronate, PEG, PECE.
Dental materials	Peptide hydrogel, hydrocolloids.
Augmentation materials	CMC.

Hydrogels are super absorbent polymeric materials which have significant roles in health care especially for wound treatment / protection. From healthcare points of view, hydrogel dressings have become a very interesting field of research for the development of a user friendly medical device for mankind.

The water holding capacity and permeability are the most important characteristic features of a hydrogel. The disintegration and/or dissolution could happened if the network chain or cross-links are degradable [7]. The Biodegradable hydrogels containing labile bonds, therefore advantageous in applications such as tissue engineering, wound healing and drug delivery. The labile bonds can be broken under physiological conditions either enzymatically or chemically, in most of the cases by hydrolysis [8,9]. Biocompatibility is the third most important characteristic property required by the hydrogel. Biocompatibility calls for compatibility with the immune system of the hydrogel and its degradation products formed, which also should not be toxic. Generally,

hydrogels possess a good biocompatibility since their hydrophilic surface has a low interfacial free energy when in contact with body fluids, which results in a low tendency for proteins and cells to adhere to these surfaces. Moreover, the soft and rubbery nature of hydrogels minimises irritation to surrounding tissue [10].

I.2. Methods to produce hydrogels

Hydrogels are broadly classified into two categories i.e. permanent / chemical gel and non permanent/reversible / physical gel. Permanent or chemical gels are covalently cross-linked (replacing hydrogen bond by a stronger and stable covalent bonds) networks [11]. They attain an equilibrium swelling state which depends on the polymer-water interaction parameter and the crosslink density [12]. Meanwhile reversible / physical gel are held together by molecular entanglements, and / or secondary forces including ionic, hydrogen bonding or hydrophobic interactions. In physically cross-linked gels, dissolution is prevented by physical interactions, which exist between different polymer chains [11]. All of these interactions are reversible, and can be disrupted by changes in physical conditions or application of stress [12]. Various hydrogels have been prepared for various applications in pharmaceutical and biomedical fields.

The general methods to produce physical and chemical gels are described below.

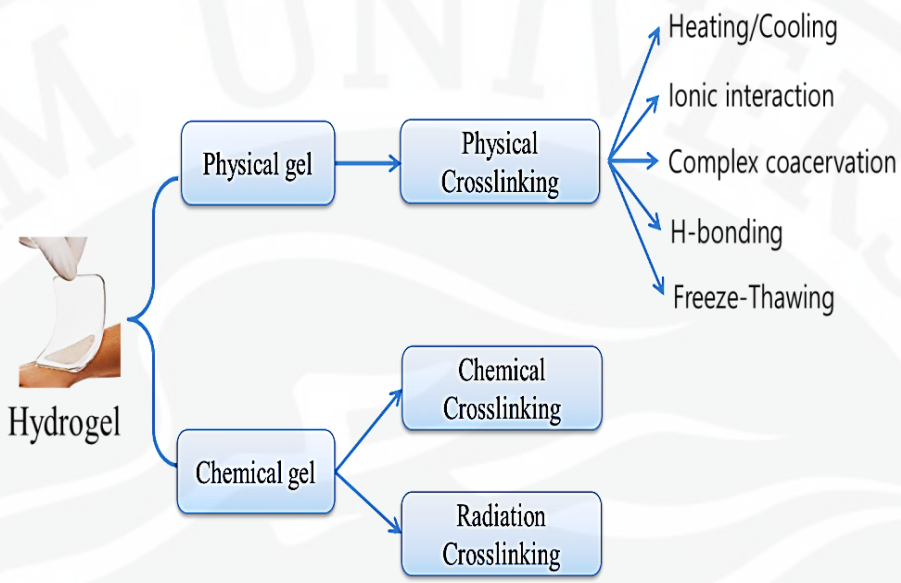

Figure 1.1. Schematic of methods for producing hydrogels

I.2.1. Physical cross-linking

The various methods reported to obtain physically cross-linked hydrogels are:

I.2.1.1. Heating/cooling a polymer solution

Physically cross-linked gels are formed when cooling hot solutions of gelatine or carrageenan. The gel formation is due to helix-formation, association of the helices, and forming junction zones [13]. Carrageenan in hot solution above the melting transition temperature is present as random coil conformation. Upon cooling it transforms to rigid helical rods. In presence of salt (K^+, Na^+, etc.), due to screening of repulsion of sulphonic group (SO^{-3}), double helices further

aggregate to form stable gels. In some cases, hydrogel can also be obtained by simply warming the polymer solutions that causes the block copolymerisation. Some of the examples are polyethylene oxide-polypropylene oxide [9], polyethylene glycol-polylactic acid hydrogel [12].

I.2.1.2. Ionic interaction

Ionic polymers can be cross-linked by the addition of di- or tri-valent counterions. This method underlies the principle of gelling a polyelectrolyte solution (e.g. Na^+ $alginate^-$) with a multivalent ion of opposite charges (e.g. Ca^{2+} + $2Cl^-$). Some other examples are chitosan-polylysine [14], chitosan-glycerol phosphate salt [15], chitosan-dextran hydrogels [12].

I.2.1.3. Complex coacervation

Complex coacervate gels can be formed by mixing of a polyanion with a polycation. The underlying principle of this method is that polymers with opposite charges stick together and form soluble and insoluble complexes depending on the concentration and pH of the respective solutions. One such example is coacervating polyanionic xanthan with polycationic chitosan [16].

I.2.1.4. H-bonding

H-bonded hydrogel can be obtained by lowering the pH of aqueous solution of polymers carrying carboxyl groups. Examples of such hydrogel is a hydrogen-bound CMC (carboxymethyl cellulose) network formed by dispersing CMC into 0.1M HCl [17]. The mechanism involves replacing the sodium in CMC

with hydrogen in the acid solution to promote hydrogen bonding. The hydrogen bonds induce a decrease of CMC solubility in water and result in the formation of an elastic hydrogel. Another example is polyacrylic acid and polyethylene oxide (PEO-PAAc) based hydrogel prepared by lowering the pH to form H-bonded gel in their aqueous solution [9].

I.2.1.5. Freeze-thawing

Physical cross-linking of a polymer to form its hydrogel can also be achieved by using freeze-thaw cycles. The mechanism involves the formation of microcrystals in the structure due to freeze-thawing. Examples of this type of gelation are freeze-thawed gels of polyvinyl alcohol and xanthan [18].

I.2.2. Chemical cross-linking

Chemical cross-linking covered here involves grafting of monomers on the backbone of the polymers or the use of a cross-linking agent to link two polymer chains. The cross-linking of natural and synthetic polymers can be achieved through the reaction of their functional groups (such as OH, COOH, and NH2) with cross-linkers such as aldehyde (e.g. glutaraldehyde, adipic acid dihydrazide). There are a number of methods reported in literature to obtain chemically cross-linked permanent hydrogels. The following section reviews the major chemical methods (i.e. crosslinker, grafting, and radiation in solid and/or aqueous state) used to produce hydrogels from a range of natural polymers.

I.2.2.1 Chemical cross-linkers

Cross-linkers such as glutaraldehyde , epichlorohydrin, etc have been widely used to obtain the cross-linked hydrogel network of various synthetic and natural polymers. The technique mainly involves the introduction of new molecules between the polymeric chains to produce cross-linked chains. Hydrogels can also be synthesized from cellulose in NaOH/urea aqueous solutions by using epichlorohydrin as cross-linker and by heating and freezing methods [19].

I.2.1.2 Chemical grafting

Chemical grafting involes the polymerization of a monomer on the backbone of polymer. The backbones are activated by the action of chemical reagent. Starch grafted with acrylic acid by using N-vynil-2-pyrrolidone is an example of chemical grafting [20].

I.2.1.3 Radiation grafting

Grafting can also be initiated by the use of high energy radiation such as gamma and electron beam. The preparation of hydrogel of CMC by grafting CMC with acrylic acid in presence of electron beam irradiation [21].

I.2.3. Radiation cross-linking

Radiation cross-linking is widely used technique since it does not involve the use of chemical additives and therefore retaining the biocompatibility of the biopolymer. Also, the modification and sterilisation can be achieved in single step

and hence it is a cost effective process to modify biopolymers having their end-use specifically in biomedical application [22]. The technique mainly relies on producing free radicals in the polymer following the exposure to the high energy source such as gamma ray, x-ray or electron beam.

I.2.3.1. Aqueous state radiation

Irradiation of polymers in diluted solution will lead to chemical changes as a result of 'indirect action' of radiation. The water radiolysis generates reactive free radicals which can interact with the polymer solute:

$$H_2O \xrightarrow{\text{Ionising radiation}} {}^{\bullet}OH, H^{\bullet}, H_3O^{+}, H_2O_2, H_2, e^{-}aq$$

The two main radicals present in saturated aqueous system react with carbohydrates (RH) by abstracting carbon bound H-atoms.

$$RH + {}^{\bullet}OH\ (H^{\bullet}) \longrightarrow R^{\bullet} + H_2O\ (H_2)$$

I.2.3.2. Radiation in paste

The cross-linking of hydrocolloids in aqueous paste-like conditions state has received significant attention recently. Under these conditions the concentration of the polymer is high such that both direct action of the radiation can form free radicals and also there is also sufficient water present to be radiolysed to form $^{\bullet}OH$ and related radicals. There is thus a high concentration of radicals in close association with the original polymer and other secondary formed polymer radicals. Thus cross-linking to form new polymers can form by way of radical-radical reaction and polymer - polymer radical reactions. If the

original polymer concentration is not sufficient to promote radical-radical reactions then degradation will result. The presence of water promotes the diffusion of macroradicals to combine and form cross-linked hydrogel network. Also, the radiolysis of water generate free radicals (hydrogen atoms and hydroxyl radicals), which increase the yield of macroradicals by abstracting H-atoms from the polymer chain [7].

I.2.3.3. Solid state radiation

Irradiation of hydrocolloids in solid state induces the radical formation in molecular chains as a result of the direct action of radiation. Here mainly two events take place (i) direct energy transfers to the macromolecule to produce macroradicals and (ii) generation of primary radicals due to the presence of water (moisture).

The application of radiation processing of synthetic polymers to introduce structural changes by cross-linking and special performance characteristics is now a thriving industry. In contrast treatment of polysaccharides and other natural polymers with ionizing radiation either in the solid state or in aqueous solution leads to degradation as described above. Therefore, a method to modify structure, without introducing new chemical groupings, could prove advantage, particularly if the process could be achieved in the solid state.

I.3. Electron Beam

Electron beam processing or electron irradiation is a process which involves using electrons, usually of high energy, to treat an object for a variety of purposes. This may take place under elevated temperatures and nitrogen atmosphere. Possible uses for electron irradiation include sterilization and to cross-link polymers.

Electron beam processing involves irradiation (treatment) of products using a high-energy electron beam accelerator. Electron beam accelerators utilize an on-off technology, with a common design being similar to that of a cathode ray television.

Electron beam processing is used in industry primarily for three product modifications:

a). The cross-linking of polymers through electron beam processing. Cross-linking is the interconnection of adjacent long molecules with networks of bonds induced by electron beam treatment. When polymers are crosslinked, the molecular movement is severely impeded, making the polymer stable against heat. This locking together of molecules is the origin of all of the benefits of crosslinking. Electron Beam processing of thermoplastic material results in an array of enhancements, such as an increase in tensile strength, and resistance to abrasions, stress cracking and solvents [23].

b). Chain scissioning or polymer degradation can also be achieved through electron beam processing. The effect of the electron beam can cause the

degradation of polymers, breaking chains and therefore reducing the molecular weight. The chain scissioning effects observed in polytetrafluoroethylene (PTFE) have been used to created fine micropowders from scrap or off-grade materials. Chain scission is the breaking apart of molecular chains to produce required molecular sub-units from the chain. Teflon (PTFE) is also Electron beam processed, allowing it to be ground to a fine powder for use in inks and as coatings for the automotive industry [24].

c). Sterilization with electrons has significant advantages over other methods of sterilization currently in use. The process is quick, reliable, and compatible with most materials, and does not require any quarantine following the processing. For some materials and products that are sensitive to oxidative effects, radiation tolerance levels for electron beam irradiation may be slightly higher than for gamma exposure. This is due to the higher doses and shorter exposure times of e-beam irradiation which have been shown to reduce the degradative effects of oxygen [24].

Irradiation creates free radicals which will often chemically react in various ways, sometimes at slow reaction rates. The free radicals can recombine forming the crosslinks. The degree of crosslinking depends upon the polymer and radiation dose. One of the benefits of using irradiation for crosslinking is that the degree of crosslinking can be easily controlled by the amount of dose. Other subtle influences include the additives in the base polymer and the type of

radiation used (related to the dose). Another influence which may not be as subtle is oxidation during irradiation. This effect will be more predominant when using gamma irradiation as compared to the much faster electron beam irradiation process. Furthermore, oxidation can continue after irradiation causing changes in properties with time. This oxidation process may reduced by antioxidants added to the polymer resin.

Ionizing radiations are divided in the most general form into two types : photon and corpuscular radiations. They are also called high energy radiations, in contrast to low energy radiations, i.e. those with a particle energy of up to about 50 eV: they are the visible light and UV radiation. UV radiation interacts with the substance in the primary stages by the mechanism of excitation of its atom and molecules, whereas high energy radiation mainly induced an ionization mechanism, leading to the formation of ions with different signs.

Photon radiations used in the chemistry of high energies are X-rays and γ-rays. In the radiation chemistry of polymers, photon radiation with a particle energy of 10^3-10^6 eV is generally used.

Corpuscular radiation include fluxes of charged particles, fast (accelerated) electrons, protons, multicharged ions and neutrons. Radioactive isotopes emit corpuscular radiation in the form of α-particles (helium nuclei) and β-particles (electrons).

In the radiation chemistry of polymers , neutron radiation is not generally

used because ‘ induced radioactivity may appear in the irradiated object as a result of nuclear reactions, although their cross section is small.

It should be noted that in the most general from γ radiation and accelerated electron are the main types of ionizing radiation used in radiation chemistry of polymers. The parameter of quantitative evaluation of the retarding ability of the medium is the energy loss per unit path of particle (or beam), the so-called linear energy transfer (LET), LΔ :

$$L\Delta = dE_{LET} / dl$$

Where dE_{LET} is the energy transferred to the substance by the charged particle along the elementary path (dl).

The absorbed dose of ionizing radiation (absorbed dose or dose) D is the ratio of the mean energy, dE transferred by ionizing radiation to the substance in an elementary volume to the mass, dm, of the substance in this volume.

$$D = dE/dm$$

According to SI, its unit of measurement is the gray (Gy) : 1 Gy is equal to the absorbed dose of ionizing radiation at which energy of ionizing radiation of 1 J is transferred to a substance of mass 1 kg.

$1\ Gy = 1\ J/kg = 6.24 \times 10^{15}\ eV/g = 6.24 \times 10^{18}\ \rho\ eV/l$

Where ρ is the density of the irradiated substance in g/cm^3.

The range of dose used in the radiation chemistry of polymers is $10\text{-}10^6$ Gy. According to SI, the energy of ionizing particles, E and the energy of ionizing

radiation, w are expressed in Joules (J). However, it is preferable to use a non-systematic unit for E – the electron-volt,(eV). 1 MeV = 1.6 x 10^{-13} J.

Upon irradiation, and taking polyethylene as an example, crosslinking mechanism can undergo the following reactions:

1. a) The formation of excited molecules :

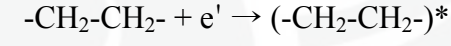

b) The ionization of molecules :

2. The formation of free radicals as a result of the fragmentation of excited molecules and ionized molecules :

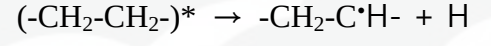

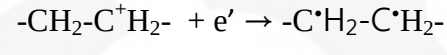

3. The interaction between the radical and polymer chain leading to the crosslinking.

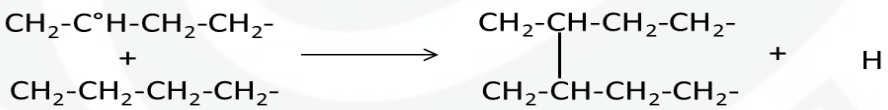

The recombination of two macroradicals leading to crosslinking,

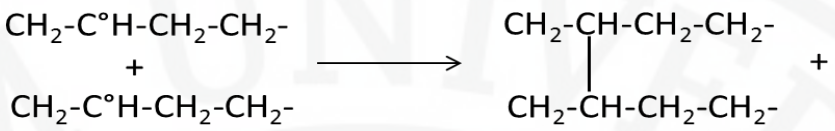

The higher the molecular weight of the polymer undergoing crosslinking, the lower is required absorbed dose [23].

I.4. The proposed methods to produce modified PEO Hydrogel films

Poly(ethylene oxide) has several advantage properties for medical applications. Among those properties i.e. biocompatible, low toxicity, water soluble polymer, antithrombogenic polymer, and nonionic polymer. Nevertheless, PEO is lacks of mechanical strength, adhesive property, cell attachment and biodegradability be applied in medical fields.

To overcome some disadvantage properties of PEO hydrogel , we try to modify PEO by adding various polymers for some purposes using an electron beam as a nontoxic and simple crosslinking method. In this work we developed the modified PEO hydrogel films using electron beam for three spesific applications i.e. wound dressing, anti-adhesion barrier and tissue engineering. We tried to find the better fabrication technique and attempt to modify PEO based hydrogel by adding certain polymer to get the appropriate properties in the certain application. There are three proposed method to develop the remarkable hydrogel for three biomedical applications.

1.4.1. Wound Dressing application

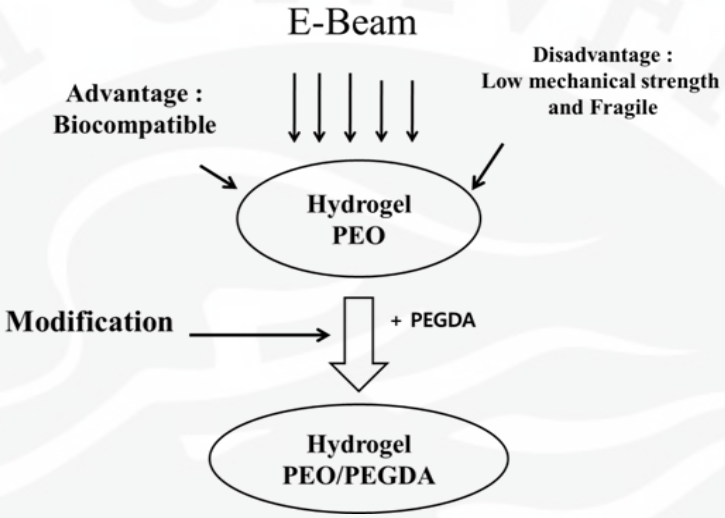

Figure 1.2. Proposed method to develop hydrogels for wound dressing

1.4.2. Anti-adhesion barrier application

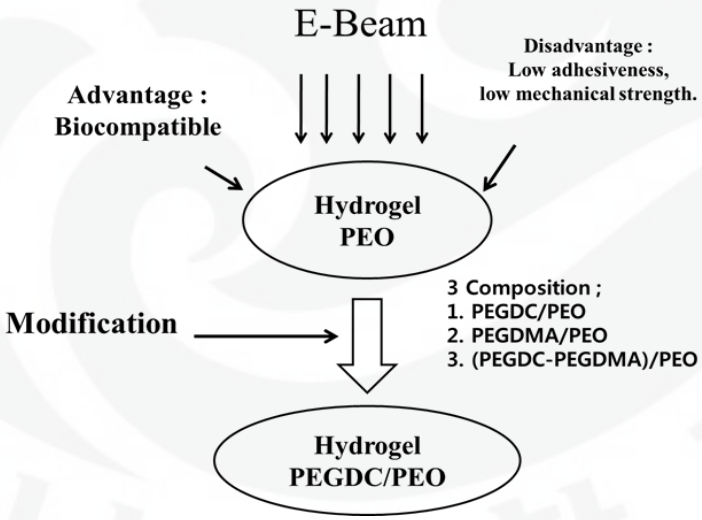

Figure 1.3. Proposed method to develop hydrogels for anti-adhesion barrier

1.4.3. Tissue engineering scaffold

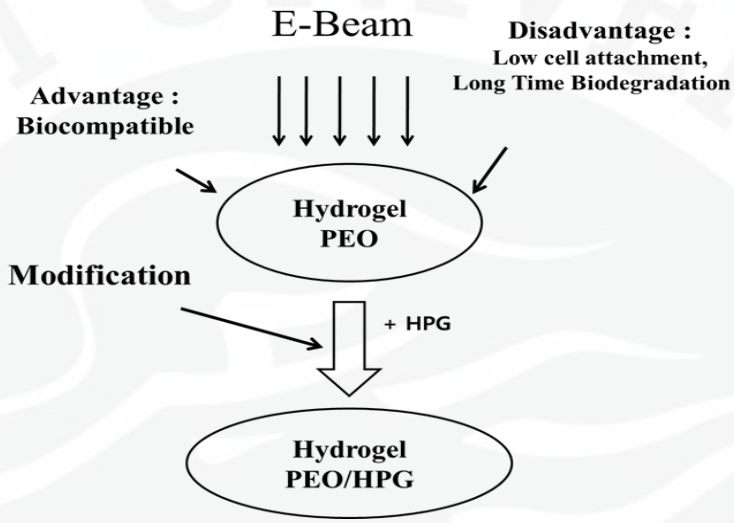

Figure 1.4. Proposed method to develop hydrogels for tissue engineering scaffold

I.5. Research objectives

To develop the facile fabrication of the remarkable modified PEO crosslinked hydrogel film which fullfilled the ideal properties of biomaterial in particular biomedical applications such as wound dressing, anti-adhesion barrier and tissue engineering scaffold using electron beam.

CHAPTER II

FABRICATION OF POLY(ETHYLENE OXIDE) HYDROGELS FOR WOUND DRESSING APPLICATION USING E-BEAM

II.1. Introduction

Wound dressing is usually used to encourage the various stages of wound healing and create better conditions for healing. They often cover the wound surface in order to accelerate its healing. The powdery hydrogel materials generally introduced to an open, draining wound in order to absorb the exudate from the wound [1]. A drawback of such hydrogel material is that the dry material can tend to clump and form lumps prior to and during introduction of the material to the wound site. Clumping can also occur after introduction of the material to the wound site. In addition, removal of lumps from the wound site without damaging the new tissue is difficult. Dressing should be easy to apply, be painless on removal, should create an optimal environment for wound healing, and should require fewer dressing changes, thereby reducing nursing time [2]. Therefore, the hydrogel having better mechanical strength is expected to be better for use as a dressing material.

In recent years, significant attention has been focused on research and development of polymer hydrogels as biomaterials, such as contact lenses, wound dressing, and drug delivery systems [3-5]. Hydrogel dressing consists of insoluble

polymers with a high water content making them an ideal dressing to facilitate autolytic debridement of necrosis and slough [6]. The hydrogel-type wound dressings can be formed by crosslinking of water soluble polymers such as polyvinyl alcohol, polyvinyl pyrolidone, polyacrilic acid, and poly(ethylene oxide) [7]. Among water soluble polymers above, poly(ethylene oxide) shows the merit of its relatively low toxicity [8,9]. However, the pure PEO hydrogel has low mechanical strength and it is very fragile [10]. Polyethylene glycol diacrylate (PEGDA) is a nontoxic, water soluble, and flexible polymer, which has polymerizable end groups [11]. PEGDA hydrogels are an attractive potential scaffold system for TEHVs because they are not only cytocompatible and modifiable but can also withstand bending deformations [12]. The biocompatible chitosan/polyethylene glycol diacrylate blend films were successfully prepared by Michael addition reaction as a potential wound dressing material which shows no cytotoxicity toward growth of L929 cell and had good in vitro biocompatibility [11]. Therefore it is expected that co-crosslinking of PEO with PEGDA with an e-beam irradiation can increase the mechanical strength and modulate other physical properties by increasing the crosslink density.

Physical, chemical, and radiation methods can be applied to preparation of the crosslinked polymer hydrogels. Among them, radiation techniques γ-ray [13] and electron beam [14] are relatively simple for improvement or modification of polymeric materials through cross-linking, grafting, and degradation reactions

[15]. However, the e-beam irradiation method is more advantageous because the radiation dose can be easily controlled and the experimental condition is straight forward for mass production of products and also the product is free from unwanted chemical impurities such as residues from initiators, retarders, and/or accelerators for initiation and for manipulation of the crosslinking reaction in chemical crosslinking methods. Moreover, the degree of crosslinking and grafting can be controlled by controlling the radiation dose [16]. When the e-beam is irradiated on a polymer film, many free radicals are generated on the polymer backbone of PEO, as the main component in a polymer blend film. The radicals attack the double bonds of PEGDA to polymerize and finally crosslink the PEGDA and PEO or the radicals undergo the chain scission reaction which reduces the molecular weight of polymer. At high temperature the viscosity of polymer is low, therefore, the radical has enough mobility to find the double bonds or another radical to make crosslinking reaction before the decay of radicals causing chain scission [17].

In this article, we demonstrate the possibility of mass production of the mechanically robust PEO hydrogel wound dressing with water permeability similar to that of a natural skin of human bodies.

II.2. Experimental Section

II.2.1. Materials

Materials. Poly(ethylene oxide) (PEO) and Poly(ethylene glycol) diacrylate (PEGDA) were purchased from Sigma-Aldrich, St. Louis, USA.

Animals. Male Sprague–Dawley (SD) rats weighting 250–280 g were purchased from Oreint Bio, (Seongnam, Korea). All rats received food and water at a temperature of 20–23℃ and a relative humidity of 50±5% for 24 h prior to the experiments. The rats were housed singly to prevent fighting and attack the wound. All animal procedures were performed according to the Guiding Principles in the Use of Animals in Toxicology, as adopted in 2008 by the Society of Toxicology. The protocols for the animal studies were approved by the Institute of Laboratory Animal Resources of Yeungnam University.

II.2.2. Preparation of crosslinked hydrogel film for wound dressing

Poly(ethylene glycol) diacrylate (PEGDA) (Mn = 700) and various molecular weights of poly(ethylene oxide) (PEO), Mn = $2x10^5$, $4x10^5$, $6x10^5$ were used for preparation of the hydrogel. Aqueous solution of PEO (8 % w/w) was prepared by stirring the solution at room temperature for 24 hours. The composition of PEGDA/PEO was changed from 0/100, 2.5/100, 5/100, 7.5/100, and 10/100 (w/w), respectively. The calculated amount of aqueous solution was poured into a petri dish to form dry PEO film with a thickness of 0.3 mm. The PEO solution was dried in the oven at 55^{o}C for 24 hours, and then remaining moisture was removed in a vacuum oven for 6 hours at the same temperature. Dry

PEO films were sealed in an evacuated polyethylene bag, followed by irradiation at various doses (100, 150, 200, 250, 300kGy) using an electron beam (EB) having a beam current of 5 mA and 10 mA with an energy of 0.7 MeV generated from an Electron Beam Accelerator.

II.2.3. Analysis

Determination of gel fraction. Immediately after irradiation, the seal was opened and the weight of the dry PEO film sample (2cmx2cm) was measured accurately. After that, the crosslinked PEO film was placed in distilled water at 50^{o}C for 24 hours for removal of the soluble parts. The insoluble gel obtained was dried in the oven at 50 ^{o}C for 24 hours and then in a vacuum oven at 50 ^{o}C for 6 hours in order to obtain a constant dry weight. The gel fraction was determined from the weight ratio between the insoluble dry gel weight and the initial weight of the polymer,

$$\text{Gel fraction} = (Wc / Wo) \times 100[\%]$$

where Wc and Wo are the weight of insoluble dry gel and the initial weight of a dry film [18].

Determination of swelling ratio. The known weight of the crosslinked dry PEO film (2cm x 2cm) was soaked in distilled water at room temperature. The weight of the swollen gel was measured at specific time intervals after removal of excessive surface water using filter papers. The procedure was repeated until there

was no further weight increase. The swelling ratio (SR) was calculated using the following equation:

$$SR = (Wt/Wo) \times 100[\%]$$

where Wt and Wo are the weight of swollen gel at time t and that of the dry PEO film, respectively [10].

Determination of the percentage increase of the size. The pieces of dry crosslinked PEO film (2cm x 2cm) was soaked in distilled water at room temperature until the film reach constant length (cm) of PEO gel. The PEO hydrogel was placed on a glass plate and then the length (cm) of PEO gel was measured. The following equation was used for calculation of percentage increase of the size (IS) :

$$IS = (L-Lo)/Lo \times 100[\%]$$

Where L and Lo are the length of swollen gel at an equilibrium state and that of the dry PEO film.

Determination of water vapor transmission rate. The water vapor transmission rate was measured using JIS 1099A standard test methods [19,20]. A round piece of crosslinked dry PEO film was mounted on the mouth of a cup with a diameter of 7 cm containing 50 g $CaCl_2$ and placed in an incubator of 90% RH at 40^{o}C. The water vapor transmission rate (WVTR) was determined as follows :

$$WVTR = ((W_2-W_1)/S) \ [g\ m^{-2}h^{-1}]$$

where W_1 and W_2 are the weight of the whole cup at the first and the second

hours, respectively, and S is the transmitting area of the sample.

Mechanical properties. The tensile strength and Young's modulus of crosslinked PEO/PEGDA hydrogel films were measured using a tensile test machine (Instron 4464,UK). The hydrogels were cut into a dumbbell shape and the mechanical properties were measured with a constant extension rate of 50 mm/min, at room temperature [21].

***In vivo* wound healing assay.** To evaluate efficacy of *in vivo* wound healing, twenty one male Sprague-Dawley rats weighing 250 ~ 280 g were selected as an animal model. The rats were devided in 3 group, 7 rats in each group. The operation was performed under the cocktail of two anesthetics, Zoletil 50® (tiletamine/zolazepam) and Rompun® (Xylazine hydrochloride), which were purchased from Virbac S.A. and Bayer, by IP injection [22] prior to the operation, the dorsal hair of rats was removed using an electric razor. Subsequently, back skin was excised for development of two full thickness wounds (1.5cm × 1.5cm). Each wound was treated with gauze (control), reference product (Medifoam H®, Ildong Pharm, Co., Korea) or test material (PEO/PEGDA dressing sheet), respectively. All materials were covered and fixed with the elastic adhesive tape, Micropore® (3M), and replaced with new ones at the proper time. Every rat was cared for in detached cages and digital images of the sites were collected every three days using a digital camera. These macroscopic data were utilized for measurement of the size reduction and the epithelizing rate using Adobe Acrobat

9 Professional ® [22-24]. Size reduction and epithelializing rate (%) were calculated as follows:

$$\text{Size reduction} = \frac{W_t}{W_0} \times 100\ [\%]$$

$$\text{Epithelializing Rate} = \frac{E_t}{W_t + E_t} \times 100\ [\%]$$

where E_t = Epithelized area on time 't', W_t = Wounded area on time 't' and W_0 = Wounded area at initial time. Multiple comparisons test was performed for statistical clarification of differences between the groups. One way ANOVA test followed by the LSD method was used for analysis of the acquired data.

Histological process. Full thickness wounded samples of skin were collected containing dermis and hypodermis, and they were crossly trimmed one part/sample based on the wounds, if possible central regions. All trimmed skins were fixed in 10% neutral buffered formalin. After paraffin embedding, sections measuring 3-4μm were prepared. Representative sections were stained with Hematoxylin and Eosin (H&E) for light microscopic examination or Masson's trichrome for collagen fibers [22,25]. Thereafter, the histological profiles of individual skin were observed under a light microscope (E400, Nikon, Japan).

Histomorphometry. For more detailed observation of histopathological changes, desquamated epithelium regions (mm), number of microvessels in granulation tissues (vessels/mm^2 of field), number of infiltrated inflammatory

cells in granulation tissues (cells/mm^2 of field), percentages of collagen occupied region in granulation tissues (%/mm^2 of field), and granulation tissue areas (mm^2/crossly trimmed central regions of wounds) were measured on prepared crossly trimmed individual histological skin samples using a digital image analyzer (DMI-300, DMI, Korea) according to previously described methods [23,24]. The histopathologist was blind to group distribution when this analysis was performed. In addition, re-epithelization rates were also calculated according to some modification, as follows [26]:

Re-epithelization

$$= \frac{\boldsymbol{Total\ length\ of\ wound(10mm) - Desquamated\ epithelium\ region(mm)}}{\boldsymbol{Total\ length\ of\ wound}} \times \mathbf{100\ [\%]}$$

Statistical analysis. A multiple comparison tests for different dose groups was performed. The Levene test was used for examination of variance homogeneity [27]. If results of the Levene test indicated no significant deviations from variance homogeneity, the obtained data were analyzed by one way ANOVA test followed by least-significant differences (LSD) multi-comparison test in order to determine which pairs of group comparison were significantly different. In the case of significant deviations from variance homogeneity observed on the Levene test, a non-parametric comparison test, Kruskal-Wallis H test was performed. When a significant difference was observed in the Kruskal-Wallis H test, the Mann-Whitney U (MW) test was performed in order to determine the specific

pairs of group comparison, which are significantly different. Statistical analyses were performed using SPSS for Windows [28]. In addition, changes between gauze control and test material treated groups were calculated in order to help the understanding of the efficacy of test materials, as follows.

Percentage changes compared with gauze control

$$= \frac{Data\ of\ tested\ group - Data\ of\ gauze\ control}{Data\ of\ gauze\ control} \times 100[\%]$$

II.3. Results and Discussion

II.3.1 Effect of dose on the gel fraction and swelling properties

Figure 2.1(a) shows the effect of irradiation dose on the gel fraction of the e-beam irradiated polymer. The gel fraction showed a steady increase, from 0.21 at 100 kGy to 0.59 at 300 kGy dose. The radicals are generally produced as a result of an indirect effect of radiation and result in crosslinking and scission reaction of polymer chains when the polymer films are irradiated with high doses of radiation. The swelling ratio decreases from 3567% to 1013% with increasing dose from 100 kGy to 300 kGy due to the increase of the crosslink density, as shown in Figure 2.1(b). All films swelled rapidly in water and reached equilibrium within 10 minutes, except for 100 kGy dose, which reached equilibrium around 60 minutes. This result demonstrated that the structure with the low crosslink density could sustain much water within the gel structure, as

expected from equation [29]. The percentage increase of the size (IS) decreased with increasing doses. The percentage increase of the size was 120%, which was obtained at 300 kGy, as shown at Figure 2.1(c).

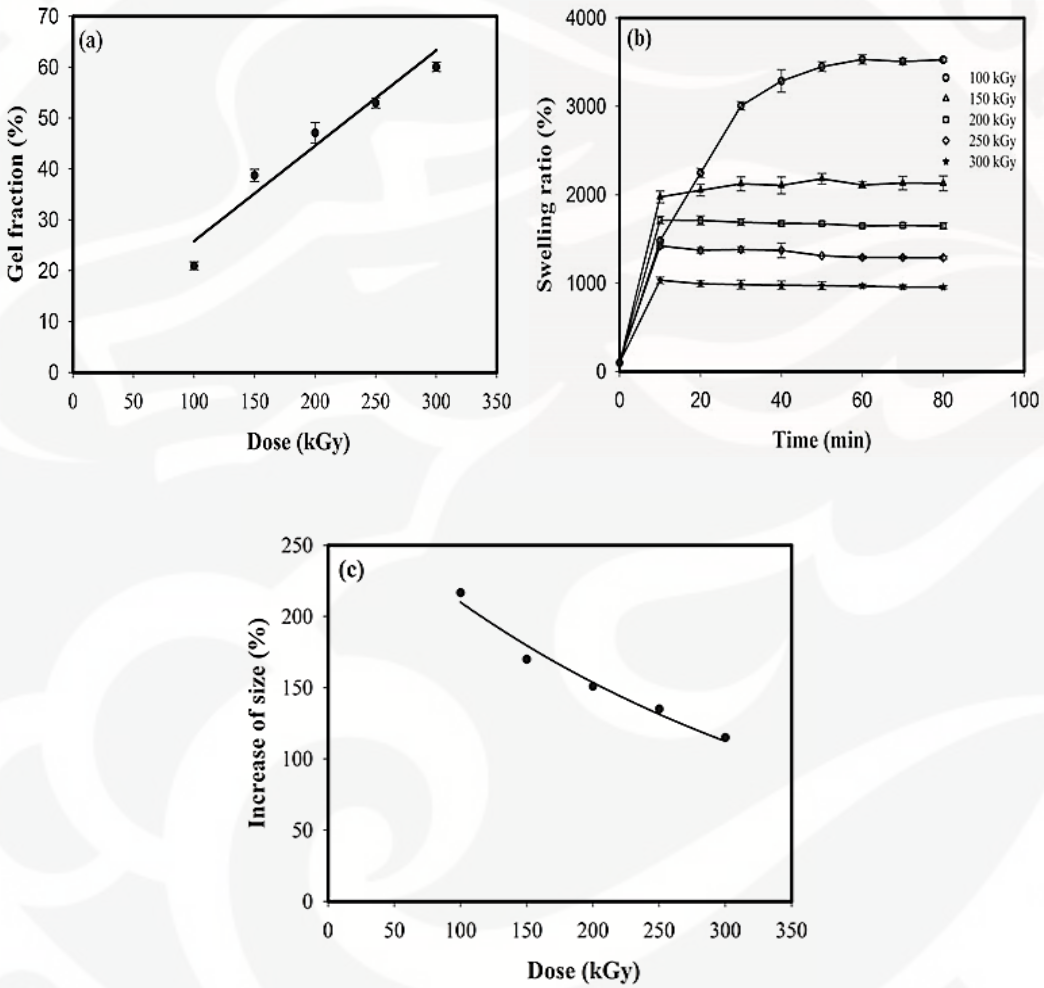

Figure 2.1. Effect of dose on (a) gel fraction, (b) swelling ratio, (c) percentage increase of the size for PEO 200,000 Mn

II.3.2 Effect of molecular weight on the gel fraction, swelling properties and size

The influence of the molecular weight on the gel fraction is shown in Figure 2.2(a). It shows that the higher the molecular weight of PEO, the higher the gel fraction was. The gel fraction showed a significant increase from 59% at 200,000 MW to 66% at 400,000 MW and then just increase slightly to 69% at 600,000 MW. The effect of the molecular weight of PEO on swelling ratio and percentage increase of the size is shown in Figure 2.2(b) and Figure 2.2(c). The swelling ratio and percentage increase of the size showed a significant decrease as the molecular weight of PEO increased from 200,000 to 400,000. Further decrease of the swelling ratio and percentage increase of the size was observed with the molecular weight of 600,000, however, the decrease was reduced. The reason for different swelling ratio and percentage increase of the size with different molecular weight may be explained as follows: although the radical density in irradiated PEO film is the same, the film with higher molecular weight may have increased physical crosslink due to the radical coupling in the polymer chains. The swelling ratio decreases from 1013% with 200,000 MW to 800% with 400,000 MW and then decrease slightly to 780% at 600,000 MW. On the other hand, Figure 2.1(b) showed that the swelling ratio decreases very significantly from 3567% to 1013% with increasing dose from 100 kGy to 300 kGy. It showed that the swelling ratio is more influenced by irradiation dose than by the

molecular weight of PEO.

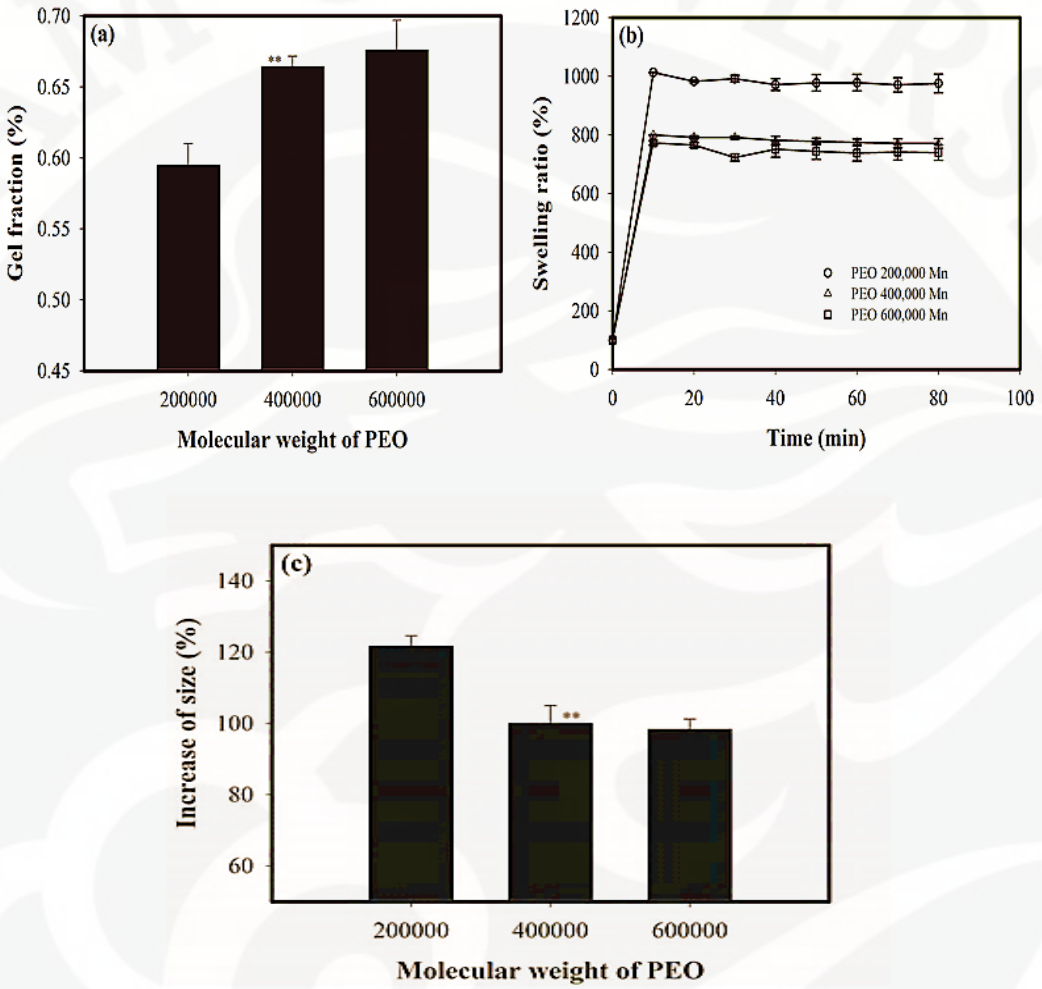

Figure 2.2. Effect of Molecular weight on (a) gel fraction, (b) swelling ratio, (c) percentage increase of the size.

According to the result above, the maximum gel fraction and the minimum swelling ratio were reached at a dose of 300 kGy with the molecular weight of 400,000. However, when the molecular weight of PEO increased, the dissolution

of PEO in distilled water was very poor due to increased viscosity. Therefore, medium molecular weight of PEO (400,000) was used to make PEO and PEO/PEGDA film for further experiments.

II.3.3 Effect of PEGDA content on gel fraction and swelling properties

A small amount of PEGDA was added to the PEO in order to increase the mechanical strength of the e-beam crosslinked PEO. Figure 2.3(a) shows the gel fraction of PEO/PEGDA hydrogel. The result showed that the gel fraction increased almost linearly with increasing the weight percentage of the PEGDA in a mixture. The swelling ratio of PEO/PEGDA hydrogel film with various compositions as a function of swelling time is shown in Figure 2.3(b). It shows that all of the hydrogel films absorb water very rapidly and reach an equilibrium weight within 10 minutes. The swelling ratio decreased with the increasing content of PEGDA, and the equilibrium swelling ratio of the crosslinked hydrogel films decreased from 771% in the film without the presence of PEGDA to 310% in that with 10% of PEGDA. The result indicated that the higher content of PEGDA can decrease the water absorption capacity of PEO/PEGDA hydrogel due to the crosslinking of PEGDA together with radicals in PEO backbones via radical polymerization. Furthermore, PEGDA also enhanced the crosslinking reaction of the PEO/PEGDA film owing to reduced viscosity, which can enhance the coupling reaction of radicals before the radical decays into an unreactive species.The percentage increase of the size declines from 105% with pure PEO

film to 58% with PEO/PEGDA containing 10% of PEGDA, as shown in Figure 2.3(c).

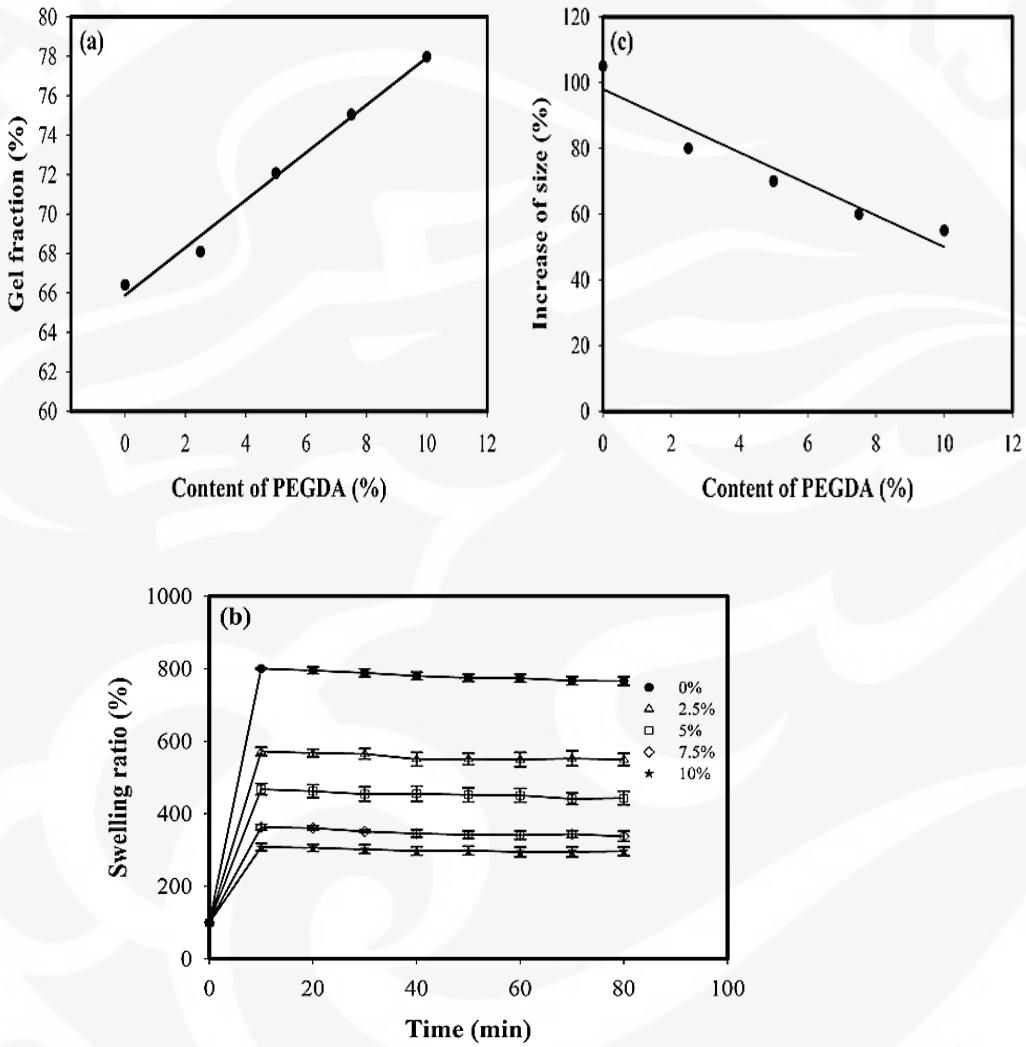

Figure 2.3. Effect of content of PEGDA on (a) gel fraction, (b) swelling ratio, (c) percentage increase of the size.

II.3.4 Effect of PEGDA content on Water vapor transmission rate (WVTR)

The effect of the content of PEGDA on the WVTR of the hydrogel is shown in Figure 2.4. The figure shows that the WVTR value is almost constant for all compositions of PEGDA because most of the matrix is PEO. The average WVTR was 19 $gm^{-2}h^{-1}$ for 2.5 – 10 % of PEGDA, however, that of pure PEO was somewhat lower, 15.89 $gm^{-2}h^{-1}$.When the value of WVTR is too high, the wound can dry rapidly, resulting in scars. In addition, if the value is too low to accumulate exudates, the healing process can be retarded, resulting in increased risk of bacterial growth [30]. Use of an ideal dressing is known to control evaporation of water from a wound at an optimal rate. The rate for normal skin is 8.5 $gm^{-2}h^{-1}$, while that for injured skin can range from 11.6 $gm^{-2}h^{-1}$ [31]. Therefore, the ideal wound dressing should have a WVTR similar or greater than 11.6 $gm^{-2}h^{-1}$. The WVTR of the PEO/PEGDA hydrogel was close to the ideal value for wound dressing.

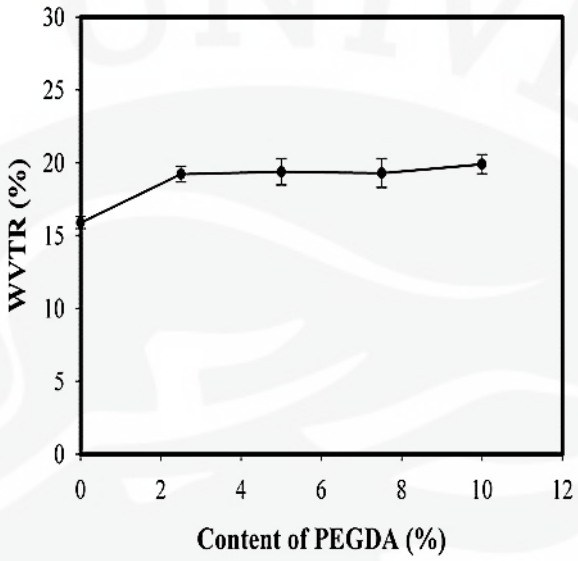

Figure 2.4. Effect of content of PEGDA on Water vapor transmission rate.

II.3.5 Effect of PEGDA content on Mechanical properties

The tensile strength of PEO/PEGDA wet hydrogel film as a function of the PEGDA content is shown in Figure 2.5. It can be seen that the tensile strength of PEO/PEGDA hydrogel increased exponentially with increasing PEGDA content due to the increased crosslink density and reached the maximum value (0.48 MPa) with 10% of PEGDA, of which strength was10 times higher than that of the pure PEO (0.044MPa). Figure 2.6 shows the Young's modulus of the PEGDA/PEO films. The Young's modulus increased even more rapidly with the increasing content of PEGDA.

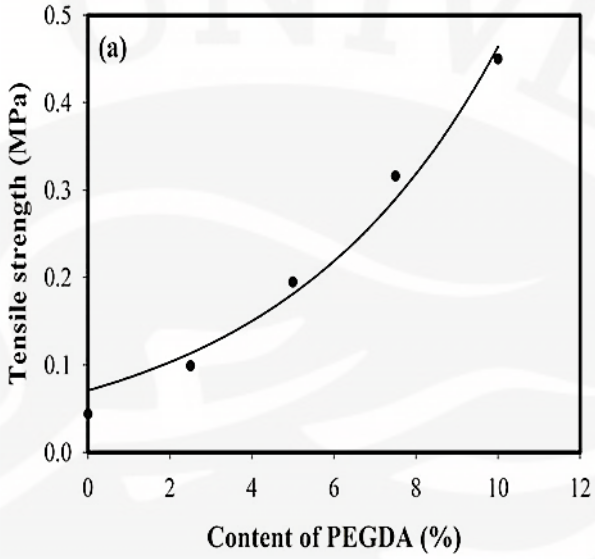

Figure 2.5. Tensile strength of PEGDA/PEO as a function of PEGDA content.

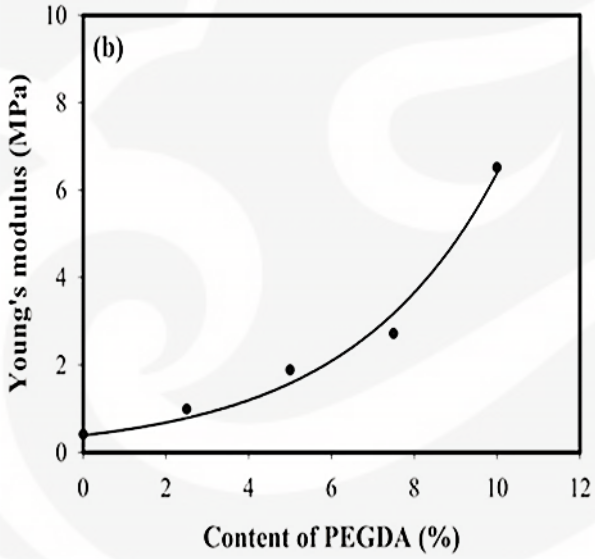

Figure 2.6. Young's modulus of PEGDA/PEO films as a function of PEGDA content.

II.3.6 *In vivo* wound healing

All animals survived until the sacrifice and there was no evidence for necrosis of epidermal tissue. Slight inflammation and bleeding were detected throughout the experiment. Each representative macroscopic data on wounds is shown in Figure 2.7 on the third postoperative day, highly severe inflammation was detected in every group of wounds. In particular, hemorrhage was accompanied in the wounds to which sterile gauze only was applied. In addition, the control group showed a dry surface and scabs, whereas the reference and the test material exhibited a moist surface. On the sixth postoperative day, reference and test material-applied wounds showed enhanced size reduction. However, the gauze-applied wounds showed lower size reduction. After the 12^{th} postoperative day, considerable closure of wounds was discovered in the reference and the test material-applied wounds, whereas comparatively large exposure was still detected in gauze-applied wounds ($p<0.05$, Figure 2.8). In addition, the trend of enhanced epithelization was observed mainly in the reference and test material-applied groups. In the same way, both epithelizing rates of the test material and the reference were significantly ($p<0.01$ or $p<0.05$) higher than that of gauze control (Figure 2.9). The test material and the reference displayed equivalent wound-healing effects in both size reduction and epithelizing rate and showed significantly improved efficacy, compared with gauze control.

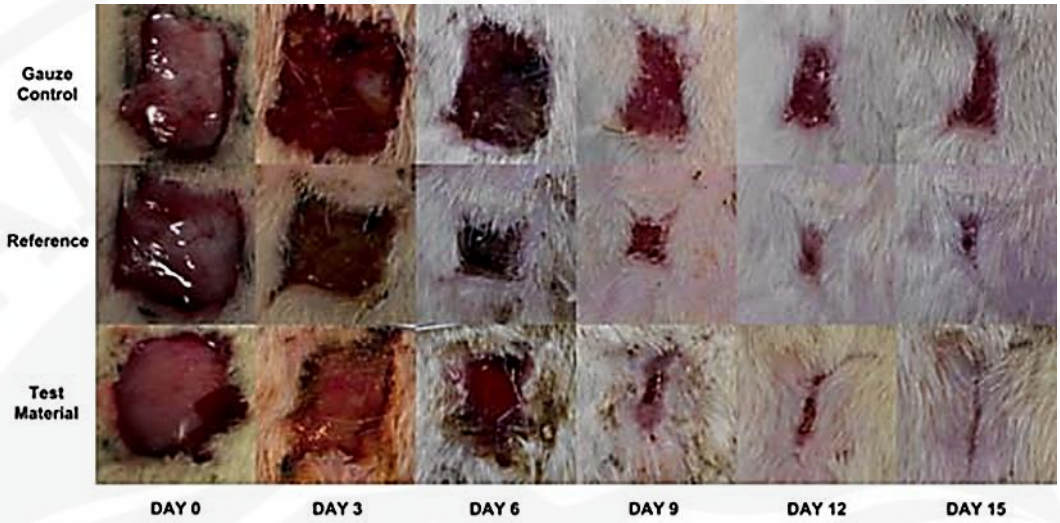

Figure 2.7. Representative macroscopic data of wounds treated with gauze control, reference and test material on day 0, 3, 6, 9, 12 and 15, respectively.

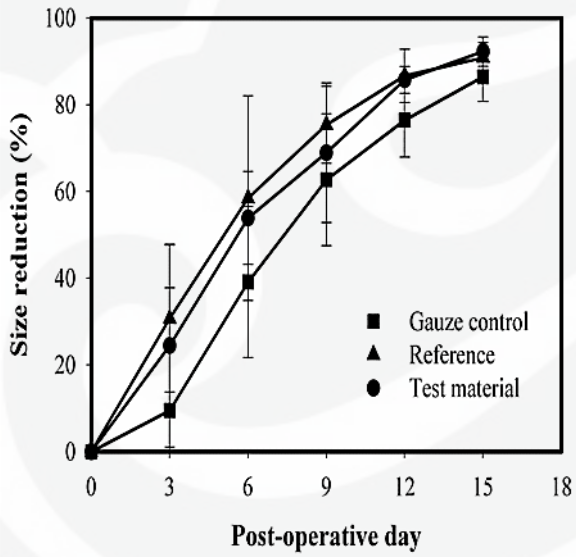

Figure 2.8. Size reduction (%) profiles of gauze control (■), reference (▲), test

material (●). *; p<0.05 as compared with gauze control group.

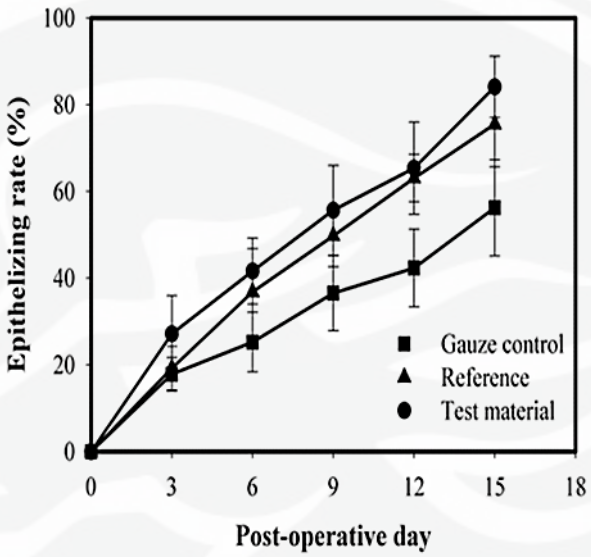

Figure 2.9. Epithelizing rate (%) profiles of gauze control (■), reference (▲), test material (●). *; p<0.05 as compared with gauze control group. †; p<0.01 as compared with gauze control group.

II.3.7 Histopathological analyses

The histomorphometrical changes on the full thickness wounds of rat dorsal back skin-desquamated epithelium regions, re-epithelization, number of microvessels (neovascularization), infiltrated inflammatory cells and percentages of collagen occupied regions in granulation tissues, granulation tissue areas are

shown in Table 2, and the representative histological profiles of the experimental groups are shown in Figure 2.10, respectively. In histopathological and histomorphometrical comparison with gauze control, significant ($p<0.01$) decreases of desquamated epithelial regions were detected in both reference and test material-applied groups. The number of microvessels (equal to neovascularization) and inflammatory cells infiltrated in granulation tissues, and granulation tissue area itself showed a remarkable ($p<0.01$) decrease in the reference and the test material-applied wounds, as compared with gauze control, and significantly ($p<0.01$) increased collagen fibers were also observed in the reference and the test material-applied skin samples. In addition, the re-epithelization rate showed significant ($p<0.01$) improvement in both. Impressively, more favorable accelerating efficacy on the full-thickness wounds was observed in test material-applied rats. In particular, according to histopathological observations, significantly ($p<0.01$ or $p<0.05$) more rapid regeneration of wounds, more rapid reconstruction of granulation tissues (decreases of granulation tissues and increase of re-epithelization rates), lower inflammatory cell infiltration, and lower neovascularization were detected in test material-treated wounds, as compared with reference-treated wounds. In addition, more favorable collagen fiber regeneration was demonstrated in the test material-applied wounds and the percentage of acollagen occupied region in the test material-applied wounds was also significantly ($p<0.01$) enhanced, as compared

to that of the reference-treated wounds (Table 2, Figure 2.10).

Table 2. Histomorphometrical values

Histomorphometry	Gauze control	Material applied groups	
		Reference	Test material
Desquamated epithelium region (mm)	4.54 ± 1.12	2.40 ± 0.90[a]	1.05 ± 1.08[ac]
Re-epithelization (%)	54.61 ± 11.16	75.96 ± 9.04[a]	89.47 ± 10.84[ac]
In granulation tissues			
Microvessels number	120.43 ± 35.88	51.29 ± 11.48[d]	21.43 ± 7.89[de]
Infiltrated inflammatory cell number	403.86 ± 114.92	206.86 ± 27.73[d]	68.43 ± 8.56[de]
Collagen occupied region (%)	34.14 ± 3.99	49.05 ± 5.81[a]	64.47 ± 6.64[ab]
Granulation tissue area (mm^2)	64.32 ± 10.05	39.90 ± 5.19[a]	27.61 ± 5.23[ab]

Values are expressed as Mean ± S.D. of seven rat wounds

[a] $p<0.01$ as compared with gauze control by LSD test

[b] $p<0.01$ and c $p<0.05$ as compared with reference by LSD test

[d] $p<0.01$ as compared with gauze control by MW test

[e] $p<0.01$ as compared with reference by LSD test

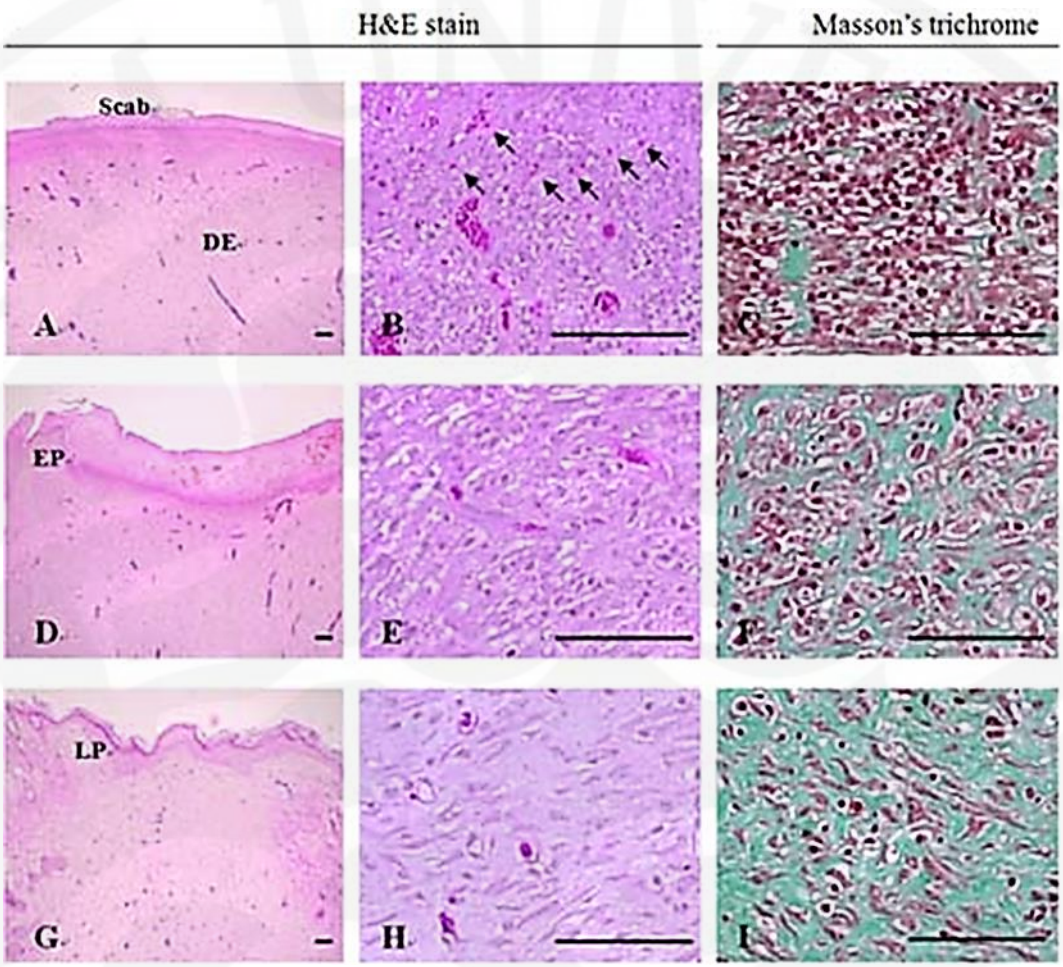

Figure 2.10. The representative histopathological profiles of full thickness skin wounds (granulation tissues) of gauze control (A~C), reference (D~F) and test material (G~I) applied rats.

Note that re-epithelization – decreases of desquamated epithelial regions, was more extendedly observed in reference and test material applied wound as compared with gauze control wound, respectively. The inflammatory cell infiltrations and neovascularization (arrows) in granulation tissues (B, E, H) in

reference and test material treated groups were also less than that of gauze control, and more numerous collagen proliferations (C, F, I; green colors) were detected in the both reference and test material applied groups as compared with gauze control, respectively. These wound healing signs were more rapidly occurred in test material applied wounds than those of reference, in this experiment.

DE, dermis; EP, regenerated epithelium, LP, lamina propria

Scale bars = 160 μm.

II.4 Conclusions

The PEO/PEGDA hydrogel prepared by e-beam irradiation was nontoxic and biocompatible with high mechanical strength. The PEO/PEGDA hydrogel contained no toxic ingredients due to the absence of any organic inhibitor, accelerator, and inorganic catalyst. Moreover, the hydrogel had a water vapor transmission rate similar to that of skin, which could maintain a moist environment on the interface of the wound and dressing in order to speed up the healing process. Results of *in vivo* study implied that the test material (PEO/PEGDA) has very favorable wound healing effects; size reduction and epithelizing rate acceleration. In addition, PEO/PEGDA hydrogel film was able to successfully create amicable environments for wound healing. Histopathological studies also indicated that PEO/PEGDA hydrogel film enhances re-epithelization

and normalization of wounded sites. These findings were considered direct evidence that PEO/PEGDA hydrogel film definitely facilitated the wound healing. Therefore, the results confirmed the possibility of commercializing robust PEO/PEGDA gel type wound dressings using e-beam irradiation.

CHAPTER III

POLY(ETHYLENE GLYCOL) DICARBOXYLATE/ POLY(ETHYLENE OXIDE) HYDROGEL FILM CO-CROSSLINKED BY ELECTRON BEAM AS AN ANTI-ADHESION BARRIER

III.1. Introduction

The major complication in surgeries is the postsurgical adhesions triggered by inflammation or tissue trauma as an effect of a normal wound-healing process [1]. The formation of postoperative peritoneal adhesions is an important complication following gynecological and general abdominal surgery [2]. An important consequence of adhesion formation in abdominal and gynecological surgeries is the development of fibrosis that can cause an intestinal obstruction [3] and infertility [3-4]. Various types of anti-adhesion barriers have been developed to reduce adhesion formation including hydrogel [5-6].

Hydrogel has three-dimensional (3D) network structures which can absorb and retain large amount of water [7]. Crosslinks have to be present in hydrogel in order to prevent dissolution of the hydrophilic polymer chains in a wet environment [8]. Various techniques have been developed to create hydrogels including physical crosslinking [9-12], chemical crosslinking [13-15], and irradiation crosslinking [16-20].

Poly(ethylene oxide) (PEO) based hydrogels, due to their significant water

content, possess a degree of flexibility similar to a soft tissue, therefore, they have good biocompatibility with low toxicity and have been exploited in many fields such as tissue engineering [21-25], drug delivery [26-30], wound dressing [31,32] and an anti-adhesion barriers [33]. Nevertheless, the pure PEO hydrogel is very fragile and it has low mechanical strength in a wet condition [32] and is lack of keeping in contact with tissue [34]. In addition, it has been considered as a biocompatible but non-biodegradable polymer [35].

Poly(ethylene glycol) dicarboxylate (PEGDC) basically contains polyethylene glycol (PEG) and two carboxylic acid groups with two polymerizable double bonds [36]. The carboxyl group improved the adhesive strength to the tissue [37,38]. Poly(ethylene glycol) dimethacrylate (PEGDMA) is nontoxic and water soluble, which also has polymerizable double bonds and degradable ester groups at the end of a polymer. It has been used in medical application for various functions such as oral insulin delivery [39] and bone regeneration application [40]. However, few research has been conducted on this material for anti-adhesion barrier film.

Chemical, and radiation methods can be applied for the production of the crosslinked hydrogels with strong bond [41]. In the chemical method, crosslinking reaction takes longer time [42] and needs the addition of chemical initiator and other additives during the polymerization. However, the additives are usually less biocompatible than the polymer matrix. An electron beam (EB)

irradiation is relatively simple for the improvement or modification of polymeric materials through cross-linking, grafting, and degradation reactions [32]. Moreover, the radiation dose can be easily controlled and the experimental condition is simple for mass production of products. In addition, the product is free from undesirable chemical impurities such as residues from initiators, retarders, and/or accelerators for initiation and manipulation of the crosslinking reaction in chemical crosslinking methods [43,44].

Co-crosslinking of PEO with PEGDC or PEGDMA can enhance the mechanical properties by increasing the crosslink density due to the existing double bonds in crosslinker molecules. In addition, the content of carboxyl groups in PEGDC is also expected to improve the tissue adherence for keeping hydrogel film in contact with tissue as well as to physically crosslink the polymer network.

In this study, we prove the possibility of the facile production of excellent hydrogel films with high mechanical properties, good biodegradability, adequate tissue adherence and low hemolysis activity for an anti-adhesion barrier.

III.2. Experimental section

III.2.1. Materials

Poly(ethylene oxide) (PEO) (M_n 6 x 10^5), poly(ethylene glycol) (PEG) (M_n 3350), maleic anhydride (M_w 98.06), poly(ethylene glycol) dimethacrylate (PEGDMA) (M_n 750), Dulbecco's modified Eagle’s medium (DMEM), 3-(4,5-

dimethylthiazol-2-yl)-2,5-diphenyl tetrazolium bromide (MTT), fetal bovine serum, and penicillin-streptomycin were purchased from Sigma-Aldrich, St. Louis, USA. Mouse fibroblast cells (NIH3T3) were purchased from ATCC (manassas, VA, USA) and Live/Dead viablility/cytotoxicity kits were purchased from Life Technology, Invitrogen, USA.

III.2.2. Synthesis of PEGDC

PEGDC was synthesized by dissolving 3.35 g of PEG in 25 ml of tolune in 2 necked flask and the stirred solution was dried at 130 °C by purging nitrogen for 1 hour. After cooling, 0.196 g of maleic anhydride was added and the reaction mixture was stirred for 18 hours at 80 °C under N_2 atmosphere. The toluene was then removed by vacuum evaporation at 85 °C under reduced pressure. The crude product was dissolved in small amount of methylene chloride and then precipitated three times into diethyl ether to remove unreacted maleic anhydride. The precipitate was then dried in the oven at 50 °C for 6 hours [36].

III.2.3. Characterizations of PEGDC

The purified PEGDC was analyzed by ^1H NMR (600 MHz, Bruker Advance DRX500) using TMS as an internal standard and $CDCl_3$ as a solvent.

III.2.4. Cytotoxicity test of PEGDC

MTT (3-(4,5-dimethylthiazol-2-yl)-2,5-diphenyl tetrazolium bromide) assay was applied to check metabolic activity of the cells on PEGDC films and control-2D. NIH3T3 cells of a mouse fibroblast cell line were grown in Dulbecco's modified Eagle's medium (DMEM) (Invitrogen, Carlsbad, CA) that contained 10% fetal bovine serum (FBS) (Invitrogen, Carlsbad, CA) and 1% penicillin–streptomycin (Invitrogen, Carlsbad, CA) at 37 °C in a humidified atmosphere of 5% CO_2. Cells (1 x 10^4) were seeded overnight on the 24-well cell culture plates and incubated for an additional 1 day, 3 days, 5 days and 7 days. Briefly, 500 µl of MTT solution (5 mg/ml, Sigma Chemicals) was added to each well and incubated for 4 h at 37 °C. The supernatant was aspirated, and the MTT-formazan crystals, produced by metabolically viable cells, were dissolved in 1500 µl of DMSO solvent. The absorbance was measured using a microplate reader at a wavelength of 490 nm. Cell viability was also investigated using a Live/Dead staining assay on 1 day and 7 days. Ethidium bromide (2 mM) was diluted in 10 ml distilled tissue culture grade PBS in combination with 4 µM of calcein acetoxymethyl ester (calcein AM) from stock solution. The working solution of the stain 100-150 µL was added and incubated for 30 min and labelled cells were observed under Nikon fluorescent microscope [45].

III.2.5. Preparation of hydrogel films

PEO and PEGDC (and/or PEGDMA) were used for preparation of the

hydrogel films. Aqueous solution of PEGDC/PEO (5% w/w) was prepared by stirring the solution at room temperature for 24 hours. The composition of PEGDC/PEO was changed from 0/100, 2.5/100, 5/100, 7.5/100, and 10/100 (w/w), respectively. The calculated amount of aqueous solution was poured into a petri dish to form dry PEGDC/PEO film with a thickness of 0.1 mm. The PEGDC/PEO solution was dried in the oven at 55 °C for 24 hours, and then remaining moisture was removed in a vacuum oven for 6 hours at the same temperature. Dry PEGDC/PEO films were sealed in an evacuated polyethylene bag, followed by irradiation at various doses (100, 150, 200, 250, 300 kGy) using an EB having a beam current of 5 mA and 10 mA with an energy of 0.7 MeV generated from an EB Accelerator. The optimum dose and composition were used to prepare three different compositions of hydrogel films, namely 10% PEGDC, 10% PEGDMA and 5% PEGDC-5% PEGDMA with the same procedure.

III.2.6. Analysis

Determination of gel fraction. Immediately after irradiation, the sealed film was opened and the weight of the dry film (2cm x 2cm) was measured accurately. After that, the crosslinked hydrogel film was placed in distilled water at 50 °C for 24 hours for removal of the uncrosslinked soluble parts. The obtained insoluble gel was dried in the oven at 50 °C for 24 hours and then in a vacuum oven at 50 °C for 6 hours in order to obtain a constant dry weight. The gel fraction

was determined from the weight ratio between the weight of an insoluble dry gel and the initial weight of a dry film using the following formula:

Gel fraction = (Wc / Wo) x 100 [%]

where Wc and Wo are the weight of insoluble dry gel and the initial weight of a dry film [46].

Determination of swelling ratio. The known weight of the crosslinked dry hydrogel film (2 cm x 2 cm) was soaked in distilled water at room temperature until the film reached the equilibrium weight. The weight of the swollen gel was measured at different swelling time intervals after removal of excessive surface water using filter papers. The procedure was repeated until there was no further weight increase. The swelling ratio (SR) was calculated using the following equation:

SR = (Wt/Wo) x 100 [%]

where Wt and Wo are the weight of swollen gel at time t and that of the dry film, respectively.

Mechanical properties. The tensile strength and the elongation at break of crosslinked hydrogel films were measured using a tensile test machine (Instron 2710-105, USA) with a constant extension rate of 10 mm/min, at room temperature.

Tissue adhesion. Tissue adhesion testing was performed using a tensile test machine (Instron 2710-105, USA). 1 inch wide and 7 inch length test strip of hydrogel film was prepared, bent back on itself, and joined together with a half inch strip of masking tape. The specimen forms a tear drop shaped loop. The taped end of the specimen loop was inserted into the upper grips. The test fixture was placed in the lower grip of the tensile tester. The tensile tester was activated so that the crosshead moves downward until the specimen loop completely contact to the 1 square inch of moist bovine intestine for 5 minutes. The maximum force required to remove the specimen loop from bovine intestine was recorded as the measure of a film adherence to the intestine [47].

Hemolysis assay. In this experiment, a dry hydrogel film was equilibrated in normal saline water (0.9% NaCl solution) for 24 hrs at 37 °C. Human ACD (acid citrate dextrose) blood (0.25 ml) was added onto the hydrogel film. After 20 min, 2.0 ml of saline was added onto the hydrogel film to stop hemolysis and the sample was incubated for 60 min at 37 °C. Positive and negative controls were obtained by adding 0.25 ml of human ACD blood and saline solution, respectively, to 2.0 ml distilled water. Incubated samples were centrifuged for 45 min; the supernatant was taken and its absorbance at 545 nm was recorded using a UV-Vis Spectrophotometer (Carry 5000, Varian, USA). The percentage of

hemolysis was calculated using the following relationship:

Hemolysis (%) = (A test sample – A(-) control)/(A(+) control – A(-) control) x 100 (3)

where A is an absorbance [48].

The student's t test was used to compare the means of each treatment group with each other in hemolysis assay, mechanical properties and tissue adhesion testing. A p value < 0.05 was considered significant. All results were reported as mean ± standard deviation (n=3).

Animal study. This study was performed with assistance from the Yeungnam university, school of medicine. The animal care and use committee of Yeungnam university approved the methods described. Twenty Sprague dawley rats weighting 240 to 270 g were used for this study. All rats were housed in an environment of 12-h-day and 12-h-night condition at standard temperature (22℃) in 2 weeks. They were fed with standard laboratory food and tap water ad libitum. All rats were anesthetized with ketamine hydrochloride and xylazine hydrochloride intramuscularly.

A midline laparotomy incision measuring 4 cm was created and the cecum was identified. The ventral side of cecum was then abraded with thermal cautery until a burn area reached approximately 2 cm^2 (1 X 2 cm). Rat in the first group

received 6 cm^2 (2 X 3cm) 10% PEGDC film barrier which was placed between the burned area and peritorium. Rat in the second group was treated with polyaxmer (Guardix-SG®, Genewel, Sungnam, Korea) in same manner. All animals, the burned area and the abdominal wall were approximated with a 4/0 Vircryl® (Ehticon Endo surgery, Inc., Cincinnati, Ohio, USA) in order to induce adhesion as cecum was too floopy. The laparotomy incision was closed with 4/0 black silk (Ailee, Pusan, Korea) suture. All rats were allowed to receive tap water and food ad albitum one day later.

All animal were euthanized via carbon dioxide inhalation on postoperative 21st day and examined for adhesion formation by two surgeons in a double-blinded manner. Adhesion criteria were classified according Avital et. al.'s study(Table 3.1) [49].

Table 3.1. Adhesion severity based on adhesion grade and percent of injured cecal surface area.

Severity	Grade	% area involved
Absent	0	0
Moderate	1	1~100
	2	1~100
	3	< 100
Severe	3	100

Grade

0 = no adhesions; 1 = thin filamentous, easily separated adhesions; 2 = thick adhesions, difficult to dissect, do not tear organ when separated; 3 = thick adhesions, not dissectible, tears organ when separated.

III.3. Results and Discussion

III.3.1. NMR characterization of PEGDC

The powder of PEGDC was analyzed based on the ^{1}H NMR ($CDCl_3$, 600 MHz) spectra results (Figure 3.1). These results show the presence of characteristic peaks that correspond to δ 3.6-3.31 (m, CH_2CH_2O, 60H), 4.3 (s, CH_2OCO, 4H), 6.2 (d, CHCHCOO, 2H), 6.4 (d, CHCHCOO, 2H).

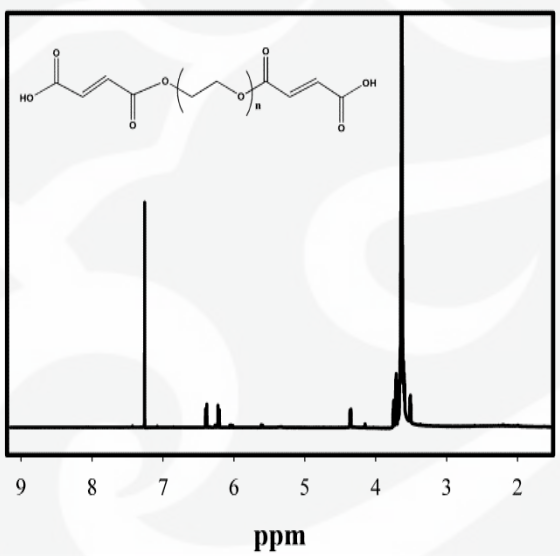

Figure 3.1. NMR spectrum of PEGDC.

III.3.2. In vitro cytotoxicity assay of PEGDC

Since the polymers are to be used for biomedical applications, the issue of

cytotoxicity is critical. Cells were found to be viable and metabolically more active in PEGDC than in control-2D. Initially, cells cultivated on PEGDC and control-2D was equal. Cells metabolic activity increased with increasing time in the presence of PEGDC indicating biocompatible nature of film as shown in Figure 3.2. Cell viability was further examined by Live/Dead staining assay, in which live and dead cells emitted green and red fluorosence, respectively. The viability of cells in the presence of PEGDC remains high after 7 days of incubation, as presented in Figure 3.3, confirming the very low toxicity of the synthesized PEGDC polymers toward fibroblast NIH3T3 cells. More dead cells were seen in control which could be due to space constrain. It is well-known that cell stops growing when it comes in contact with adjacent cell and since 2D has limited space hence more dead cells are observed. PEGDC film provides 3D support with larger surface area which allows cell to proliferate for longer period of time.

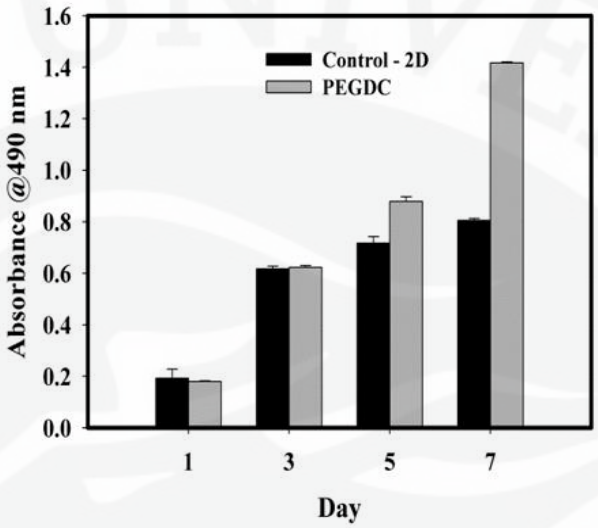

Figure 3.2. Results of MTT assay which indicate total metabolic cells at any given time interval.

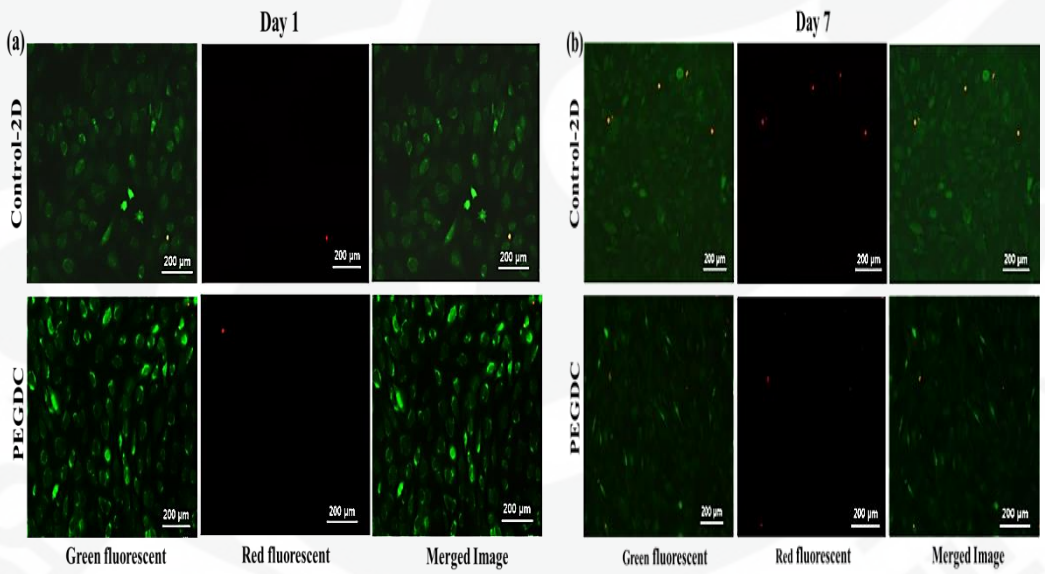

Figure 3.3. Fluorescent images of NIH3T3 fibroblast cells. a,b, Live/Dead staining performed on 1st and 7th days respectively.

III.3.3. Effect of dose on the gel fraction and swelling properties

Figure 3.4(a) shows the effect of irradiation dose on the gel fraction of the crosslinked film containing 5% of PEGDC. The gel fraction showed a steady increase, from 31% at 100 kGy to 79% at 300 kGy dose. The EB irradiation generates radicals on polymers and crosslinkers which make crosslinking between PEGDC and PEO matrix polymer chains. The swelling ratio decreased from 1468% to 744% with increasing dose from 100 kGy to 300 kGy due to the increase of the crosslink density as shown in Figure 3.4(b). All films swelled rapidly in water and reached equilibrium within 5 minutes. This result demonstrated that the structure with the low crosslink density could sustain much water within the gel structure, as expected from equation [50].

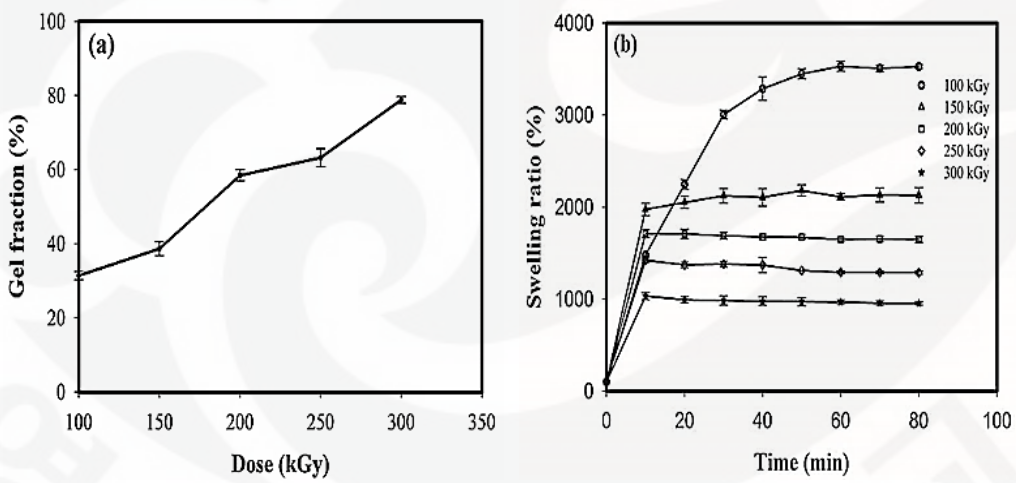

Figure 3.4. Effect of dose on (a) gel fraction, (b) swelling ratio

III.3.4. Effect of PEGDC content on gel fraction and swelling properties

Figure 3.5(a) shows the gel fraction of PEGDC/PEO hydrogel. The result showed that the gel fraction increased linearly with increasing the weight percentage of the PEGDC in a mixture. The swelling ratio of PEGDC/PEO hydrogel film with various compositions as a function of swelling time is shown in Figure 3.5(b). The swelling ratio decreased with the increasing content of PEGDC, and the equilibrium swelling ratio of the crosslinked hydrogel films decreased from 876% in pure PEO film to 641% in the film containing 10% of PEGDC. The result indicated that the higher content of PEGDC can decrease the water absorption capacity of PEO/PEGDC hydrogel due to the crosslinking of PEGDC together with radicals in PEO backbones via radical polymerization. In addition, PEGDC seemed to enhance the crosslinking reaction of the blend film owing to reduced viscosity during EB irradiation, which may enhance the coupling reaction of radicals before the radical decays into an unreactive species.

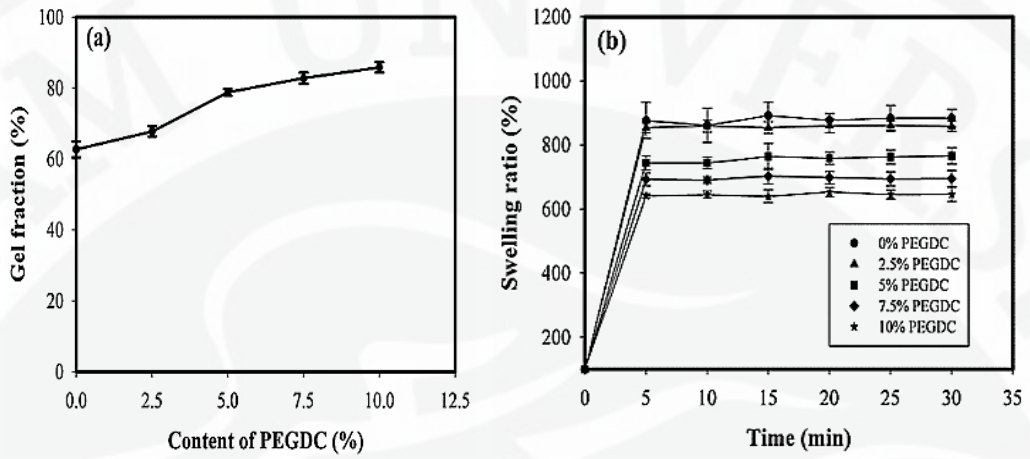

Figure 3.5. Effect of content of PEGDC on (a) gel fraction, (b) on swelling ratio.

III.3.5. Mechanical properties

The tensile strength of wet hydrogel film as a function of the composition is shown in Figure 3.6(a). It can be seen that there was no significant difference of the tensile strength in the 10% PEGDC in comparison with 5% PEGDC-5% PEGDMA ($p = 0.1095$), although there was a significant difference with 10% PEGDMA ($p=0.0307$). All hydrogels showed high tensile strength in a range from 1.84 ± 0.11 MPa to 2.13 ± 0.07 MPa which is much higher than the tensile strength of oxiplex films (0.017 MPa) [51] or methyl cellulose gel (0.16 MPa) [52] due to the high crosslink density of hydrogels. However, the elongation at break of 10% PEGDC showed a significantly higher level in comparison with 10% PEGDMA ($p=0.0053$) and 5% PEGDC-5% PEGDMA ($p=0.0096$) as seen in

Figure 3.6(b). The result indicates that 10% PEGDC hydrogel has better mechanical strength for biomedical application such as an anti-adhesion barrier with good ductility. The unexpected ductility result might be due to the -COOH groups which may make physical crosslinking points by intermolecular H-bonding.

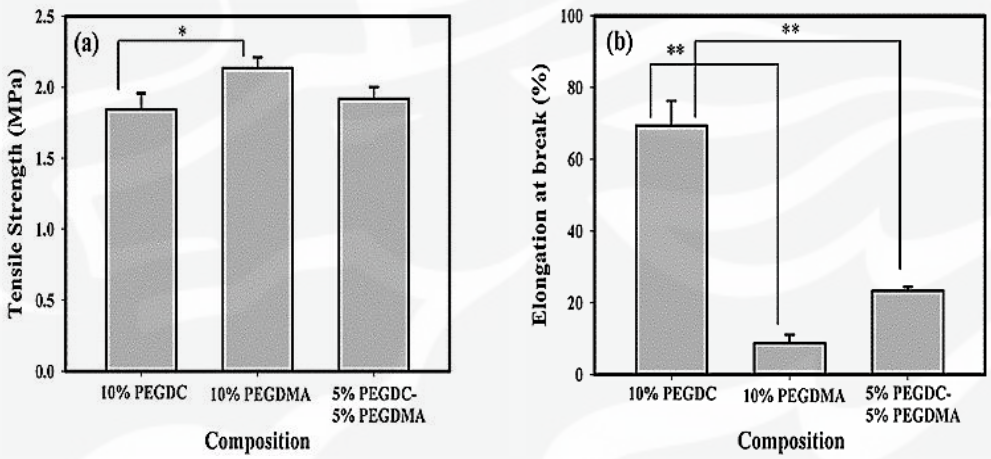

Figure 3.6. Effect of composition of hydrogel film on (a) tensile strength, (b) elongation at break (n = 3, *p < 0.05, **p<0.01).

III.3.6. Tissue adhesion

The adherence of a hydrogel film on the tissue could be critical to avoid tissue adhesion during the wound healing process to ensure that the film was easily placed onto tissue with an adequate adherence. The tissue adhesiveness of wet hydrogel film was determined by measuring the peak detachment force

required to separate the film from the bovine intestine. As shown in Figure 3.7, the force recorded for tissue adhesiveness increased significantly in the 10% PEGDC group in comparison with 10% PEGDMA (p=0.0139) or 5% PEGDC-5% PEGDMA (p=0.0146). The highest peak detachment force (75.67 ± 1.15 cN) obtained at 10% PEGDC was 50% higher than that of pure PEO (50 cN) [38]. Therefore, the result proved that the carboxyl group in PEGDC affects the tissue adherence of hydrogel films and makes the film stick to the bovine intestine better via a wet adhesion mechanism. This improvement is essential for the use of PEO as the main compound for an anti-adhesion barrier because pure PEO has low tissue adhesion property [38].

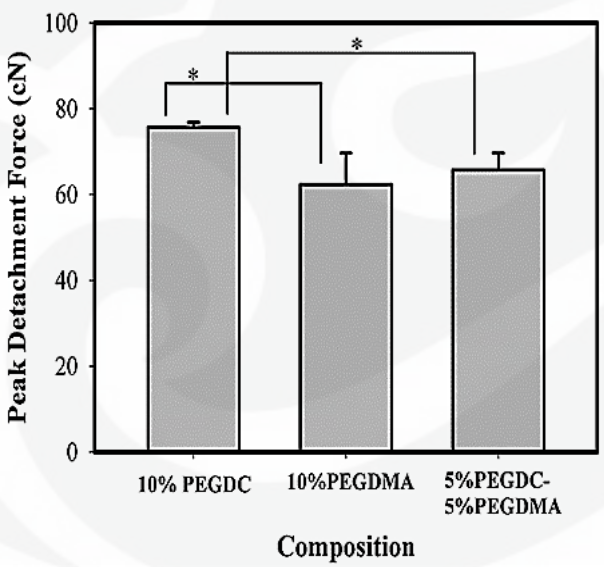

Figure 3.7. Peak Detachment Force of hydrogel film as a function of composition (n = 3, *p < 0.05, **p<0.01).

III.3.7. Hemolysis assay

Test was performed to analyze the blood compatibility of hydrogel films. In the hemolysis assay, the percentage of hemolysis in the 10% PEGDC was significantly lower than that of 10% PEGDMA (p=0.0083) or 5% PEGDC-5% PEGDMA (p=0.0087) (Figure 3.8). The low hemolysis activity of 10% PEGDC (6.03 ± 0.01%) indicated better blood compatibility with respect to other composition. Figure 3.8 shows that 10% PEGDC hydrogel film has the lowest hemolysis activity (6.03 ± 0.01%) which indicates better blood compatibility with respect to other composition. The hemolysis result proved that the PEGDC hydrogel film is a potent candidate for *in vivo* medical application.

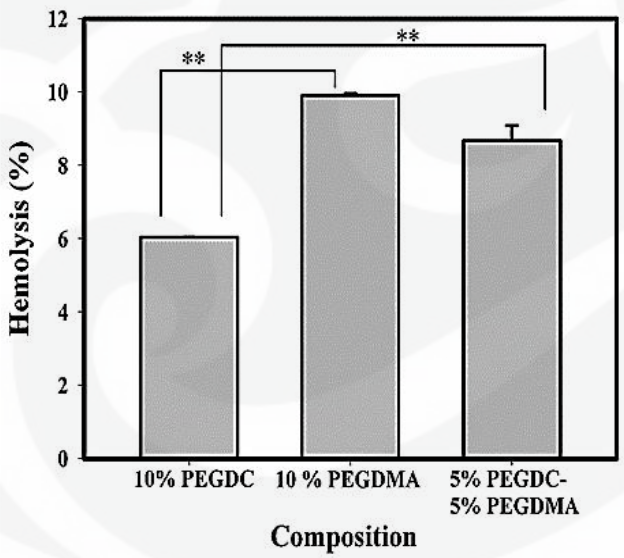

Figure 3.8. Percentage of hemolysis of hydrogel films (n = 3, *p < 0.05, **p<0.01).

III.3.8. Animal study

Base on the superiority of hydrogel film in mechanical properties, tissue adhesion and hemolysis assay, we used 10% PEGDC as anti-adhesion barrier films in the animal study. Three rats died in first postoperative day due to cecal perforation. There was no wound infection, sepsis, dietary deficiency to affect the results. After three additional animal studies with 20 animals, 10 were treated with Guardix-SG® and the other 10 were treated with 10% PEGDC hydrogel films. All of the hydrogel film with 10% PEGDC degraded *in vivo* within three weeks. The result was surprising considering that PEO has been believed as a non-biodegradable synthetic material [35]. It is still under investigation but the crosslinking reaction of PEO with crosslinkers might have increased the biodegradation of the PEO matrix.

The grade of adhesions and the percentage of an injured cecal surface area for all animals are given in Table 3.2. The frequency of adhesion severity with the 10% PEGDC group was less than those of Guardix group as seen in Figure 3.9. The grade of an adhesion was assigned according to the former research [49]. The hydrogel with 10% PEGDC showed better *in vivo* results as expected from mechanical tests and tissue adhesion experiments. 60% of rats in the 10% PEGDC group had no adhesions between the cecum and the abdominal wall, which is somewhat better than the Guardix group with 50% no adhesion, while both materials have the same level (10%) of severe adhesion. However, the Guardix

showed larger surface area of adhesion on the cecal wounds. The inferior results of the commercial product, Guardix-SG®, seemed to be due to the fast dissolution of a hydrogel on the wound surface as a result of lack of chemical crosslinking.

Table 3.2. The adhesion degree and the percentage of injured cecal surface area for all animals.

Rat		1	2	3	4	5	6	7	8	9	10
Guardix-SG®	grade	1	1	2	3	2	0	0	0	0	0
	area	1	1	5	5	4	0	0	0	0	0
10% PEGDC	grade	0	0	2	1	0	0	3	0	1	0
	area	0	0	5	1	0	0	5	0	1	0

Area

0 = 0% area involved; 1 = 1 ~ 24 % area involved; 2 = 25 ~ 49 % area involved; 3 = 50 ~ 74% area involved; 4 = 75~ 99 % area involved; 5 = 100 % area involved.

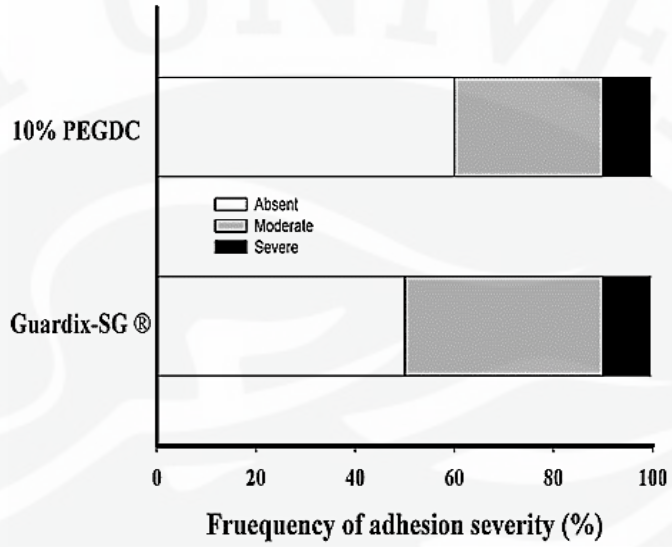

Figure 3.9. Adhesion severity of 10% PEGDC hydrogel and Guardix-SG® group.

III.4. Conclusions

The novel crosslinked PEO and PEGDC (or PEGDMA) hydrogel was developed using an electron beam irradiation as an anti-adhesive barrier material. All compositions exhibited high tensile strength, however, the film with 10% of PEGDC showed highest elongation at break (69.33 ± 6.87%) which is required for good film handling characteristics during surgical operation. The tissue adherence of the crosslinked hydrogel film reached the maximum value with 10% PEGDC. The result also indicated that the carboxyl group in PEGDC enhanced the tissue adherence of hydrogel films on the bovine intestine. In the hemolysis assay, 10% PEGDC also showed the better hemolysis activity (6.03 ± 0.01 %)

than 10% PEGDMA or 5% PEGDC-5% PEGDMA. As expected from physical properties of 10 % PEGDC, the 10% PEGDC hydrogel films demonstrated good anti-adhesive effect compared to Guardix-SG® in animal study. In addition, all of the hydrogel films with 10% PEGDC degraded within three weeks which indicates that crosslinked PEGDC/PEO hydrogel film is biodegradable *in vivo*. Therefore the crosslinked PEGDC/PEO hydrogel film proved to be the potent biomedical materials as an effective anti-adhesive barrier with superior properties such as biodegradability, low toxicity, low hemolysis activity and good ductility.

CHAPTER IV

HYPERBRANCHED POLY(GLYCIDOL) / POLY(ETHYLENE OXIDE) HYDROGELS CROSS-LINKED BY E-BEAM AS MICROPOROUS SCAFFOLDS FOR TISSUE ENGINEERING APPLICATIONS

IV.1. Introduction

Various approaches currently used to engineer tissues depend on material scaffolds that serve as extra cellular matrices (ECM) to organize cells into a three-dimensional architecture, which directs the growth of a desired tissue [1]. Development of porous scaffolds for engineering applications has been of interest recently [2-5]. However, adequate manufacturing techniques must be developed to enable proper attachment and proliferation of cells of a particular tissue in the porous scaffolds, and such techniques should allow proper control of the levels of porosity and pore size [3]. These physical properties must be tailored to meet the requirements of the particular tissue under consideration to provide mechanical stability and space for tissue expansion [4].

Porous three dimensional (3-D) scaffolds that direct tissue formation have received a great deal of attention in tissue engineering applications. These scaffolds must possess specific surface characteristics, such as a balance between hydrophilicity and hydrophobicity of matrix polymers, to promote cell adhesion. In addition, scaffolds should have adequate mechanical properties to introduce the

3-D structure and gradually degrade when the new tissue and an extracellular matrix are formed. Many conventional techniques are available to generate 3-D scaffolds for tissue engineering applications, such as solvent casting, gas foaming, particulate leaching and electrospinning [6,7]. However, these technologies all have some limitations, such as difficulty controlling pore size and producing an interconnected porous structure for cell growth.

Hydrogels have been studied intensively and used as tissue engineering scaffolds because they can provide a highly swollen 3-D environment similar to tissues and allow diffusion of nutrients and cellular waste through the elastic networks [8,9]. Various techniques have been developed to create hydrogels, including physical cross-linking [10], chemical cross-linking [11], and irradiation cross-linking [12,13]. Their biocompatibility and viscoelastic properties make them suitable as templates to engineer tissues, and they have been used to repair and facilitate regeneration of a variety of tissues, including skin, cartilage, bone and vasculature [14-16].

Poly(ethylene oxide) (PEO) is currently FDA approved for several medical applications and is one of the most commonly applied synthetic hydrogel polymers for tissue engineering. Due to their significant water content, PEO based hydrogels possess a degree of flexibility similar to a tissue. Therefore, they have good biocompatibility with low toxicity and have been exploited in many fields, including tissue engineering [17-19], drug delivery [20-22], wound dressing [23]

and an anti-adhesion barriers [24,25]. PEO and chemically similar poly(ethylene glycol) (PEG) are hydrophilic polymers that can be photocrosslinked by modifying each end of the polymer with either acrylates or methacrylates [26,27]. Hydrogels are then formed when the modified PEO or PEG is mixed with the appropriate photo initiator and cross-linked via UV exposure [26,28].

However, PEO or PEG hydrogels typically exhibit minimal or no intrinsic biological activity due to the nonadhesive nature of PEO or PEG chains [29]. It should be noted that anchorage-dependent cells encapsulated in PEG hydrogels show low viability due to the bio-inert characteristic of PEG [30,31]. Researchers have developed a variety of modified bioactive PEO/PEG hydrogels to mimic the natural ECM [32,33]. Hyperbranched poly(glycidol) (HPG) is a flexible hydrophilic aliphatic polyether polyol prepared in branched forms that was found to have very good biocompatibility based on a variety of *in vitro* and *in vivo* assays [34].

Electron beam (e-beam) irradiation is a relatively simple method for the modification of polymeric materials through cross-linking, grafting, and degradation reactions [35]. Moreover, the radiation dose can be easily controlled and the experimental condition is simple [23,36]. In addition, the product is free from undesirable chemical impurities such as residues from initiators for initiation and manipulation of the cross-linking reaction in chemical cross-linking methods [37]. In this study, we demonstrated facile fabrication and easy control of the

morphology and porosity of HPG/PEO tissue engineering scaffolds using e-beam irradiation.

IV.2. Experimentals section

IV.2.1. Materials

Poly(ethylene oxide) (PEO) (M_n 6 x 10^5), trimethylol propane (M_w 134.17), potassium methoxide (M_w 70.13), glycidol (M_w 74.08), Dulbecco's modified Eagle's medium (DMEM), DAPI (4′,6-diamidino-2-phenylindole), fetal bovine serum, and penicillin-streptomycin were purchased from Sigma-Aldrich (St. Louis, MO, USA). Mouse fibroblast cells (NIH3T3) were purchased from ATCC (Manassas, VA, USA) and Presto Blue® reagents were purchased from Life Technology, Invitrogen (Calrsbad, CA, USA).

IV.2.2. Synthesis of HPG

HPG was synthesized by deprotonating 0.0175 g of trimethylol propane in potassium methoxide solution (0.007 g in 0.3 methanol). Next, 29.632 g of glycidol was added to the solution drop wise (1 mL /h), after which it was stirred (50 rpm) for 26 hours at 95°C. The sample was then allowed to cool, at which point a small amount of methanol was added to the flask to dissolve the crude product. The sample was subsequently precipitated three times in acetone to remove unreacted reactants, after which the precipitate was dried in an oven at

50°C for 1 day. The samples were then dissolved again in methanol and the Na^+ counter ion was exchanged using a cation anion exchanger. Finally, the methanol was removed by vacuum evaporation at 50°C under reduced pressure.

IV.2.3. Characterizations of HPG

The purified HPG was analyzed by FTIR (C86199 Perkin Elmer) and ^1H NMR (600 MHz, Bruker Advance DRX500) using tetramethylsilane (TMS) as an internal standard and DMSO as a solvent. ^1H NMR (600 MHz): δ (ppm) = 4.71-4.42 (OH), 3.71-3.27 (CH_2,CH), 2.51 (CH_2) (TMP), 2.07 (CH_3) (TMP); FTIR (KBr): cm^{-1} = 3410(OH), 2885(CH), 1590(CH_2), 1480(CH_3), 1061(C-O).

IV.2.4. Preparation of HPG/PEO hydrogel scaffolds

PEO and HPG were used to synthesize the hydrogel scaffold. Briefly, aqueous solution of HPG/PEO (5% w/w) was prepared by stirring the solution at room temperature for a few hours. The composition of HPG/PEO was changed from 0/100 to 10/100, 20/100, and 30/100 (w/w). Aqueous solution was poured into a petri dish to form dry HPG/PEO hydrogel with a thickness of 0.1 mm. The HPG/PEO solution was dried in the oven at 55°C overnight, after which the remaining moisture was removed in a vacuum oven for 6 hours at the same temperature. Dry HPG/PEO hydrogels were sealed in an evacuated polyethylene bag, then subjected to cross-linking by irradiating at 300 kGy using an e-beam

with a current of 5 mA and 10 mA with an energy of 0.7 MeV generated by an e-beam Accelerator.

IV.2.5. Analysis

Chemical structure analysis. Dry cross-linked HPG/PEO hydrogel scaffolds with different compositions were analyzed based on FTIR (C86199 Perkin Elmer).

Thermal properties. The glass transition (Tg) and melting temperature (Tm) of un-crosslinked hydrogel scaffolds were characterized by differential scanning calorimetry (DSC Q200, USA).

Determination of swelling ratio. A known weight of cross-linked dry film was soaked in distilled water at room temperature until the hydrogel reached equilibrium, during which time the gel was weighed at different intervals after removal of excessive surface water using filter paper. The procedure was repeated until there was no further weight increase, after which the swelling ratio (SR) was calculated using the following equation:

$$SR = (Wt/Wo) \times 100\ [\%] \quad (1)$$

where, Wt and Wo are the weight of swollen gel at time t and the dry film, respectively [24].

Determination of cross-linking density. The cross-linking density was calculated based on the Flory-Huggin theory and Flory-Rehner equation using swelling ratio data. First, the interaction parameter (χ) was calculated based on the Flory-Huggin theory, where the mixing free energy (ΔG) is a function of the volume fraction of the polymer (υ_p) and interaction parameter (χ), where the value of free energy equal to zero ($\Delta G = 0$) is the equilibrium swelling condition.

$$\Delta G = RT \{\ln(1-\upsilon_p) + \upsilon_p + \chi\upsilon_p^2\} \quad \text{(Flory-Huggin equation)} \quad (2)$$

The Flory-Rehner equation was then used to find the cross-linking density.

$$-[\ln(1-\upsilon_p) + \upsilon_p + \chi\upsilon_p^2] = N V_s [\upsilon_p^{1/3} - \frac{\upsilon p}{2}] \quad \text{(Flory- Rehner equation)} \quad (3)$$

where, N is the cross-linking density (mol/m^3) and V_s is the molar volume (m^3/mol) of the solvent [38].

Mechanical properties. The tensile strength, compressive modulus and elongation at break of cross-linked hydrogel scaffolds were measured using a tensile test machine (Instron 2710-105, USA) with a constant extension rate of 10 mm/min at room temperature for tensile strength and 0.1 mm/min for compressive modulus tests. Three samples of each composition of hydrogels were used. The compressive modulus of the hydrogels was measured with the slope of the stress-strain curve.

Morphology. The pore morphology of the hydrogels was investigated by scanning electron microscopy (SEM). Hydrogels were freeze dried for 48 h (Freeze drier Terroni, LV 2000, Brazil) prior to SEM observation. For the observations, samples were placed over an aluminum support and sputtered with gold. The micromorphology of the freeze-dried hydrogels was then evaluated by scanning electron microscopy (SEM, 4100) at 15 kV. The mean pore size of the scaffolds was determined by analysis of the corresponding SEM images. The porosity of each type of scaffold was measured by immersing the scaffolds (initial weight, Wo) into ethanol at room temperature for 24 h (wet weight, W), and then calculated using the following equation:

$$\text{Porosity}\ (\%) = \frac{(W - W_o)\rho_1}{\rho_1 W + (\rho_2 - \rho_1)W_o} \times 100\% \quad (4)$$

where, ρ_1 and ρ_2 represent the density of hydrogel and ethanol, respectively [39].

In vitro degradation. To measure the *in vitro* degradation, hydrogels were placed in a bottle filled with 30 ml of PBS solution at 37℃, after which degradation rates were measured at 0, 1, 7, 14, 21 and 28 days. The hydrogels were partly removed from the bottles at a predetermined time, rinsed thoroughly with distilled water, and dried under a vacuum at 37℃ to achieve a constant weight.

In vitro cytotoxicity. Cytotoxicity of the 3D hydrogel films was evaluated using mouse fibroblast cells. DAPI (4′,6-diamidino-2-phenylindole) staining was applied to check the metabolic activity of the cells on HPG/PEO hydrogel scaffolds. NIH3T3 cells of a mouse fibroblast cell line were grown in DMEM (Invitrogen, Carlsbad, CA) containing 10% fetal bovine serum (FBS) (Invitrogen, Carlsbad, CA) and 1% penicillin–streptomycin (Invitrogen, Carlsbad, CA) at 37℃ under a humidified atmosphere of 5% CO_2. Cells (1×10^4) were seeded overnight in 24-well cell culture plates and incubated for an additional 1, 3, 5, 7 or 9 days. The scaffolds were then harvested, washed with PBS (phosphate-buffered saline), incubated for 10 minutes in DAPI solution and observed under a fluorescent microscope (Nikon, Japan). Cell viability was also checked using Presto Blue® reagent (Invitrogen). Briefly, hydrogels used for culturing cells were incubated with 100 µl of Presto Blue for 30 minutes at 37℃, after which the absorbance was read at 570 nm. Viability was then determined based on comparison to a standard graph generated by seeding different concentrations of cells.

Statistical analysis. Experiments were performed using three samples per condition. Data are reported as mean ± standard deviation, compared by paired t test using sigma plot 10. A value of $p < 0.05$ was considered statistically significant.

IV.3. Results and discussion

IV.3.1. General scheme of cross-link formation of HPG/PEO hydrogel

It is commonly believed that the radical generated by high energy e-beam makes coupling reaction with an adjacent radical. In this work we proposed the scheme to describe the cross-linking reaction mechanism of PEO in the presence of HPG. The reactivity of radicals may different depending on the position of a polymer but the majority of blend is PEO. Therefore, the major coupling reaction between radicals could be due to the radicals on PEO backbone. Some of radicals in HPG may react with a radical in PEO backbone too as seen in Figure 4.1.

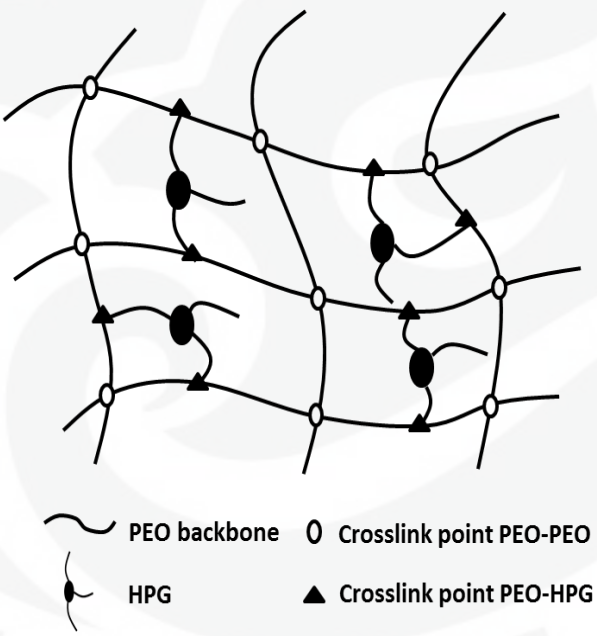

Figure 4.1. Proposed mechanism of cross-link formation of HPG/PEO hydrogel

IV.3.2. Thermal properties

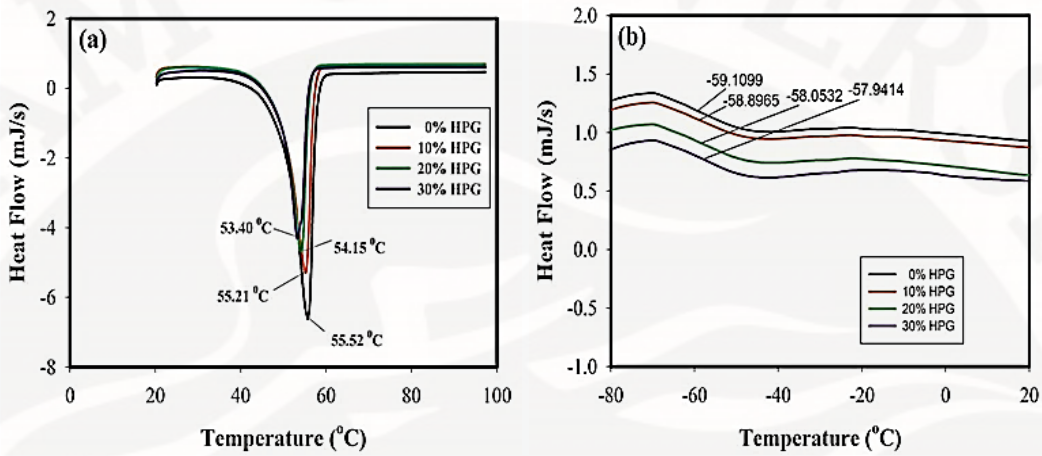

Figure 4.2. DSC measurements of uncross-linked films for various HPG contents (a) melting point, (b) glass transition point.

Thermal properties of the polymer blend may have some importance for their processing and application. Figure 4.2(a) and figure 4.2(b) show the DSC thermograms of uncrosslinked HPG/PEO blends as a function of a HPG composition. The endothermic peaks representing the melting point (Tm) of polymer blends appear in a range of 53.4°C–55.5°C. Tm decreased slightly from 55.5°C to 53.4°C as the content of HPG increased from 0 to 30%. This decrease might have been caused by the disordered state of the polymer chain, which is usually observed in miscible blends [40]. The glass transition temperature (Tg) of a matrix polymer generally decreases in the presence of low molecular miscible additives owing to the increase in free volume. However, the Tg of HPG/PEO

blends appearing in a range of -57.9°C to -59.1°C showed the opposite behavior. The increased Tg with increasing HPG might have been caused by physical crosslinking interactions such as H-bonding between OH of HPG and C-O-C of PEO. Both Tg and Tm indicated that HPG influences the thermal properties of PEO blends.

IV.3.3. FTIR characterization of HPG/PEO hydrogel scaffolds

The cross-linked and dry HPG/PEO films containing 0%, 10%, 20% and 30% of HPG were analyzed using FTIR-ATR spectroscopy (Figure 4.3). The peak at 2880 cm^{-1} was used as a reference to compare the change of the intensity of other peaks. The OH stretching peak at 3400 cm^{-1} increased with the increasing concentration of HPG. The spectra also demonstrated that most of HPG in a HPG/PEO mixture was incorporated into the cross-linked polymer network after E-Beam irradiation.

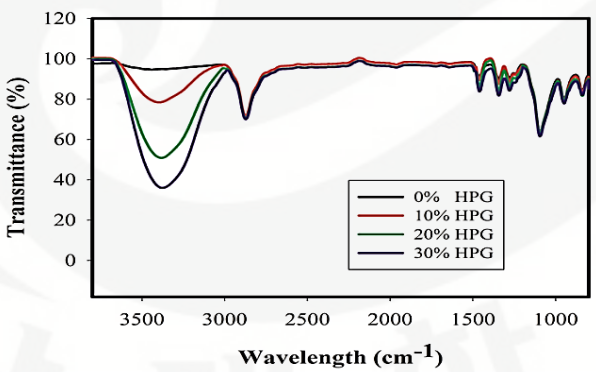

Figure 4.3. FTIR-ATR spectra of HPG/PEO cross-linked film.

IV.3.4. Effect of HPG content on swelling ratio and cross-linking density

The swelling ratio of HPG/PEO hydrogel with various compositions as a function of swelling time is shown in Figure 4.4(a). The swelling ratio increased with increasing content of HPG. Specifically, the equilibrium swelling ratio of the cross-linked hydrogel films increased from 836% in pure PEO hydrogel to 943% in hydrogel containing 30% HPG. These findings indicated that a higher HPG content can increase the water absorption capacity of the PEO/HPG network due to the hydrophilicity of HPG. Another reason for the increased swelling ratio at 30% HPG might be the reduced cross-linking density caused by the low MW of HPG. As the MW decreases, the number of radicals generated in a polymer backbone could become lower at the same irradiation dosage. Therefore, the chance of an intermolecular radical coupling reaction between HPG and PEO chains might be lower than for high MW pure PEO. Hence, the crosslink density calculated from the Flory-Rehner equation decreased slightly ($p>0.05$) in response to increasing HPG content, as shown in Figure 4.4(b). The results also demonstrated that HPG did not accelerate the cross-linking reaction as expected from increased mobility of polymer chains as inferred from thermal analysis. This was likely because, when the HPG/PEO film was irradiated with a high energy e-beam, the temperature of the sample increased to near 70°C, which is higher than the Tm of PEO. Therefore, all radicals in polymer chains have sufficient mobility to find adjacent radicals and generate a cross-linked bond.

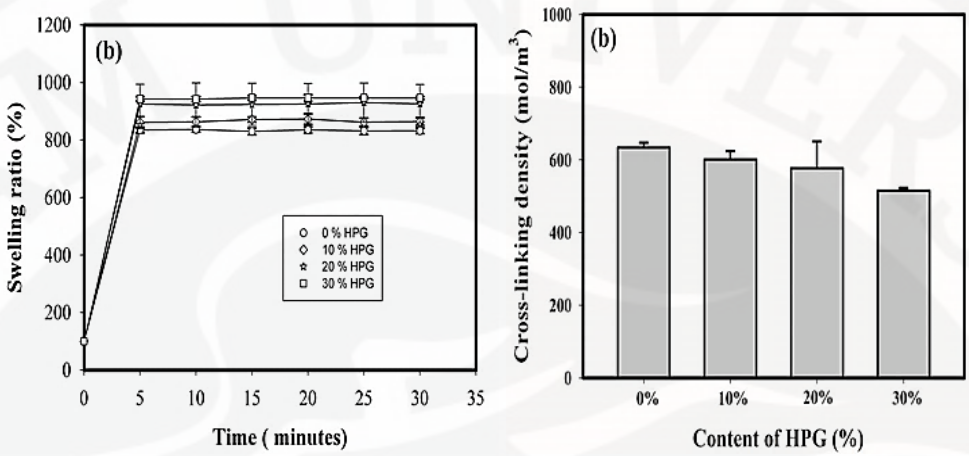

Figure 4.4. Effect of content of HPG on (a) swelling ratio and (b) cross-linking density.

IV.3.5. Mechanical properties

To determine the mechanical properties of the scaffolds, which are important for clinical operation, the tensile strength and compressive modulus of different hydrogels with different compositions were analyzed. The tensile strength of wet hydrogel as a function of composition is shown in Figure 4.5(a). As expected from the swelling ratio, there was no significant difference ($p>0.05$) in the high tensile strength of each hydrogel (approximately 0.26 ± 0.05 MPa). The value of the 30% HPG/PEO hydrogel was slightly lower than that of the others due to a low crosslinking density. The same trend was also observed for the compressive modulus ($p>0.05$), as shown in Figure 4.5(c), where all compositions

had a similar compressive modulus (1.82 ± 0.02 MPa). However, as shown in Figure 4.5(b), the elongation at break increased significantly ($p<0.05$) with increasing HPG content, with 30% HPG having the highest value (48.46 ± 1.18%). In general, hydrogel having a low crosslink density has poor mechanical properties. Therefore, these results suggest that the HPG content may have increased the elongation at break via generation of many physical crosslinks caused by H-bonding between OH groups of HPG and C-O-C groups of PEO. The resulting flexibility of scaffolds is important in clinical operations as the scaffold can be easily torn apart during surgery.

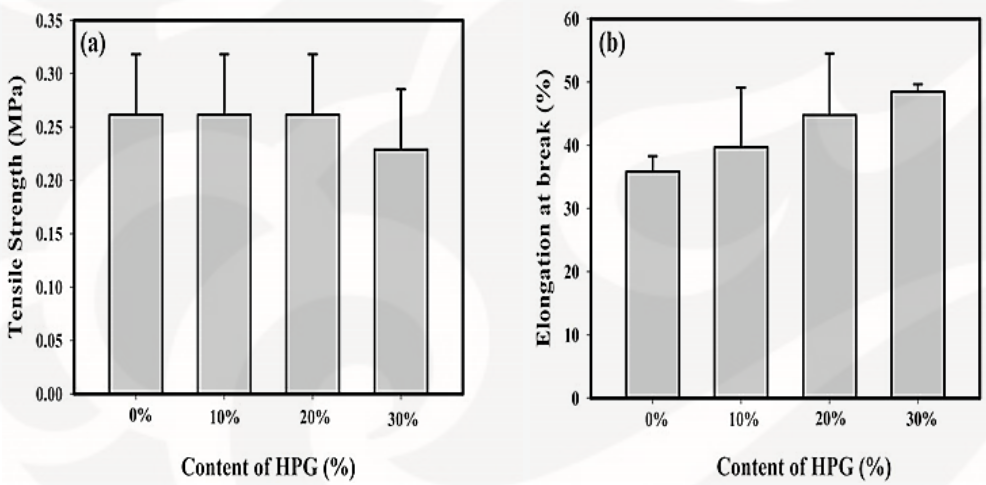

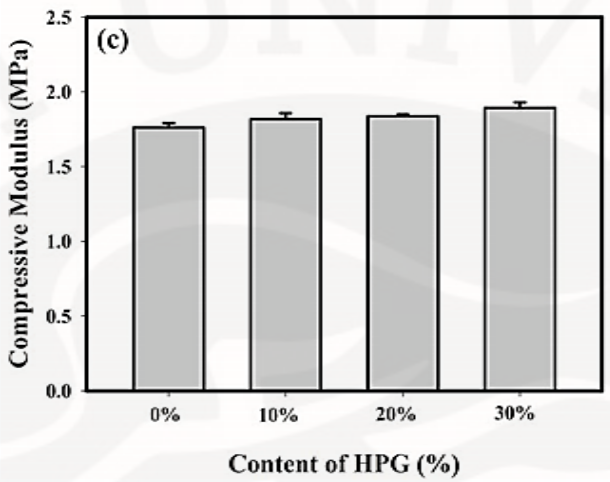

Figure 4.5. Effect of content of HPG on (a) tensile strength, (b) elongation at break and (c) compressive modulus.

IV.3.6. Morphology of HPG/PEO hydrogel

It is important to note that porosity is an important parameter to consider during tissue engineering because a highly porous structure provides a larger surface area, which increases the cell attachment to scaffolds and promotes better cell growth through easier passage of nutrients to the growing cells. In this study, the microstructure of the cross-linked HPG/PEO hydrogels was analyzed by scanning electron microscopy (SEM). As shown in Figure 4.6, the pore sizes of pure PEO scaffolds and the HPG/PEO blend system differed significantly. Once freeze-dried, the pure PEO hydrogel retracted to almost its original size due to a high crosslink density, indicating a lower porosity than expected. Conversely,

hydrogels that contained HPG showed uniform and large pore structure. The fine pore structure generated by the addition of HPG confirmed that HPG plays an important role in control of the pore size of the hydrogels. The pore size of pure cross-linked PEO was 36.2 ± 4.3 μm, which increased significantly from 69–122 μm as HPG content increased. To the best of our knowledge, porous structures with a size less than 200 μm are required for good tissue engineering scaffolds [41]. As shown in Figure 4.7, the porosity of 30% HPG was about 96.3 ± 0.7%, while slightly smaller porosities of 93.7 ± 1.2% and 92.9 ± 1.0% were obtained for 20% HPG and 10% HPG, respectively. These findings clearly indicate that hydrogels containing HPG have high porosity (>90%), which is required for high density cell seeding and supply of nutrient and oxygen [42]. Overall, these results indicate that HPG/PEO hydrogel film has a suitable pore size and porosity that is close to ideal for scaffold to be used in tissue engineering [39,43].

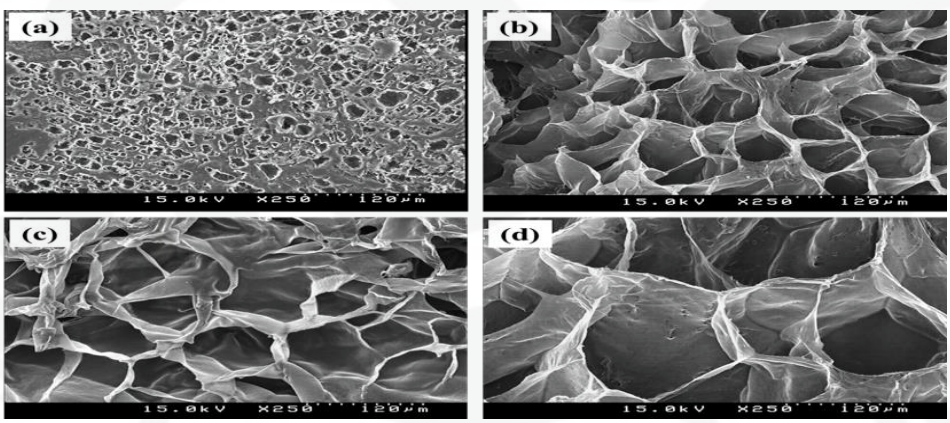

Figure 4.6. Microstructure of HPG/PEO hydrogel scaffolds (a) 0% HPG, (b) 10% HPG, (c) 20% HPG and (d) 30% HPG.

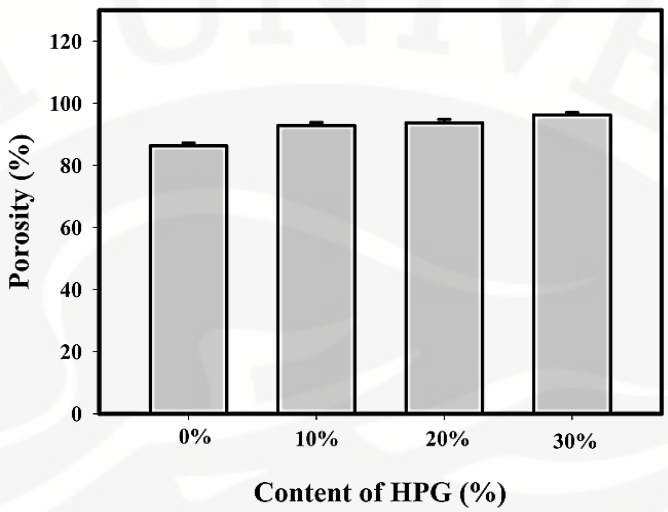

Figure 4.7. The porosity of HPG/PEO hydrogel scaffolds at various composition.

IV.3.7. In vitro degradation rate of hydrogel scaffolds

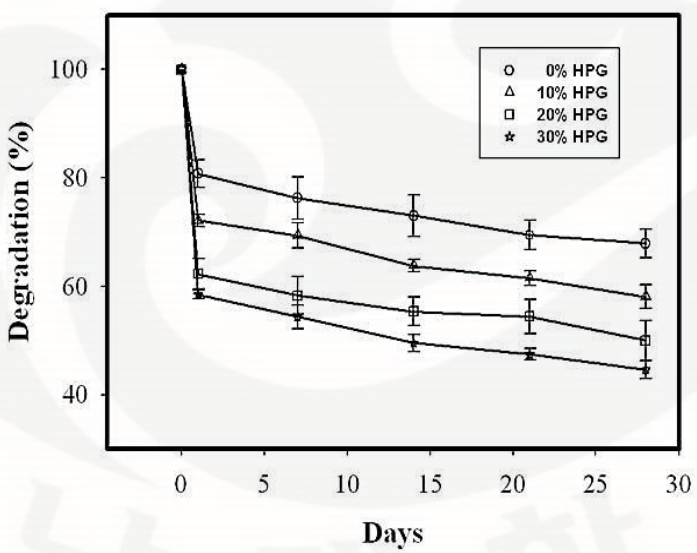

Figure 4.8. Effect of HPG content on the degradation of hydrogel scaffolds.

Our findings indicate that HPG content influences the *in vitro* degradation rate of hydrogel in PBS buffer solution. The weight of hydrogel decreased significantly on the first day, then gradually decreased within 4 weeks. As shown in Figure 4.7, a higher HPG content was associated with faster degradation, which confirms that the presence of HPG causes faster degradation of hydrogel films. The increased degradation might be due to the hydroxyl groups, which can be easily protonated as a beginning of hydrolysis. It is well known that an ideal scaffold should have a proper degradation rate to match the regeneration process of the damaged tissue [44]. These *in vitro* results of degradation of HPG/PEO hydrogel indicate that the degradation rate can be modulated simply by changing the content of HPG.

IV.3.8. In vitro cytotoxicity

The main problems associated with hydrogel application in regenerative medicine are use of chemical agents that tend to create toxic by-products upon degradation as cross-linkers. Several studies have evaluated the fabrication of hydrogels with less chemical agents to eliminate problems with cytotoxicity [45]. In the present study, hydrogel scaffolds were synthesized by e-beam irradiation without the presence of any chemical cross-linker. The images of the interaction between fibroblast cells and the scaffolds at day 1 and 3 are shown in Figure 4.8. The highest cell density at day 1 appeared in the 30% HPG hydrogel. This could

have been due to the larger pore size and uniform distribution of pores, which allowed better absorption of medium, thereby allowing easy transportation of cells and medium within the matrix. Furthermore, hyper-branched scaffold could also facilitate cellular attachment. As culture time increased, more cells were observed proliferating on the scaffolds, indicating the compatible nature of synthesized HPG. Higher concentrations of HPG in scaffolds with better cell density were observed at day 3, signifying that better biocompatibility of the scaffold could be due to the concentration of HPG. As shown in Figure 4.10, cell viability was high after 1, 3, 5 and 7 days for all compositions of hydrogel scaffolds. Furthermore, the significant increase of cell viability was observed for 30% HPG at the day 3 ($p<0.05$). The greatest decrease in cell viability was observed for 0% HPG at day 9, which may have been related to the low swelling capacity of pure PEO hydrogel and collapse of the scaffolds. Taken together, these results indicate that HPG/PEO hydrogel scaffolds produced using an e-beam exhibit good cell viability and low cytotoxicity since no potential toxic chemical agents were generated during the synthesis process.

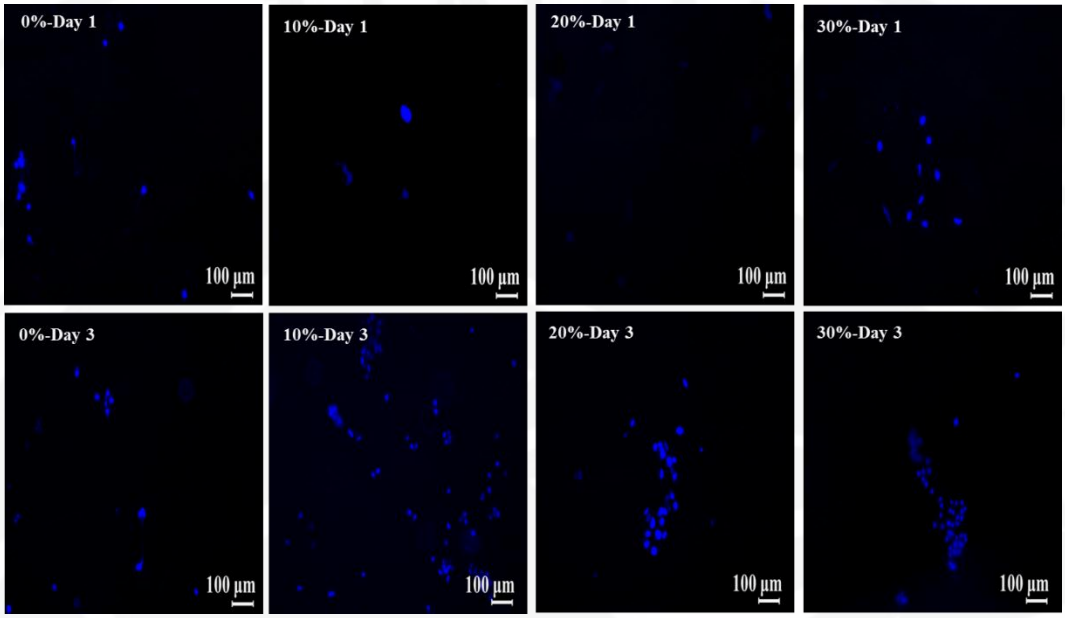

Figure 4.9. Images of fibroblasts cultured in HPG/PEO scaffolds for 1 and 3 days. The scaffolds and the cell nucleus are labeled by black and blue, respectively.

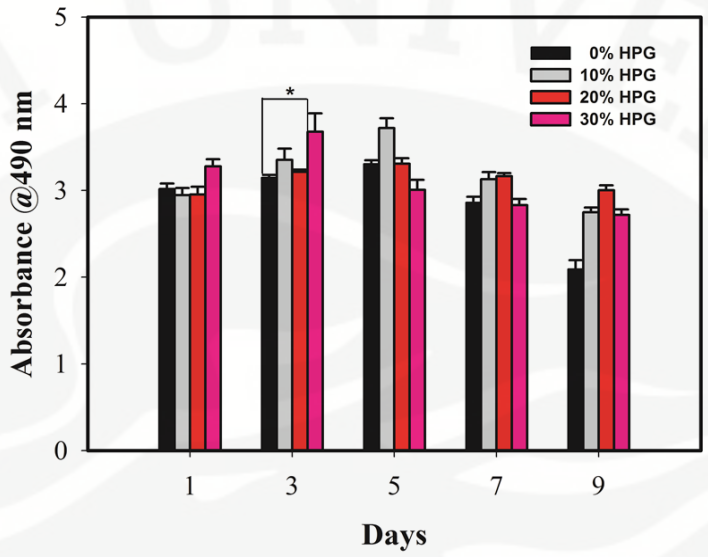

Figure 4.10. Cell viability of HPG/PEO hydrogel scaffolds at any given time interval.

IV.4. Conclusions

In this study, the microporous HPG/PEO hydrogel scaffold was successfully developed using a simple e-beam irradiation. The FTIR-ATR spectra showed that most of the HPG was incorporated into the cross-linked scaffold network. The pore size of hydrogel scaffolds fabricated by this method could be easily tailored by controlling the content of HPG in the polymer blend. The *in vitro* cytotoxicity results demonstrated that HPG/PEO hydrogel scaffolds exhibited good cell viability and low cytotoxicity, as expected from the materials. The increasing HPG content also increased the elongation at break, the swelling

ratio and the degree of degradation. Overall, these results indicate that the cross-linked HPG/PEO hydrogel has the potential for use as scaffolds for tissue engineering applications.

CHAPTER V

CONCLUSIONS AND FUTURE WORK

The development of modified poly(ethylene oxide) (PEO) hydrogel films with poly(ethylene glycol) diacrylate (PEGDA), poly(ethylene glycol) dicarboxcylate (PEGDC), and hyperbranch polyglycidol (HPG) was successfully produced with improved properties using electron beam (E-Beam) for three major applications namely wound dressing, anti-adhesion barrier and tissue engineering scaffold.

Cross-linked PEGDA/PEO hydrogel was developed for wound dressing application. The contents of the PEGDA influenced the gel fraction, swelling ratio, mechanical properties, and water vapor transmission rate. Healing under the wet environment of the hydrogel dressing was faster than with a gauze control and a commercial reference. The results demonstrate the possibility of the facile production of mechanically robust and transparent wound dressing materials with improved wound healing characteristics.

The cross-linked PEGDC/PEO and PEGDMA/PEO hydrogels were developed for an anti-adhesion barrier application. Three different compositions (10% PEGDC, 10% PEGDMA, 5% PEGDC–5% PEGDMA) were used to prepare crosslinked hydrogel films. Among them, 10% PEGDC hydrogel film exhibited the highest tissue adherence. The result also indicated that the carboxyl

groups in PEGDC affect the tissue adherence of hydrogel films via H-bonding interactions. In animal studies, 10% PEGDC anti-adhesion hydrogel film demonstrated better anti-adhesive effect compared to Guardix-SG®.

A microporous hydrogel scaffold was developed from HPG and PEO using e-beam induced cross-linking for tissue engineering applications. HPG was synthesized from glycidol using trimethylol propane as a core initiator and cross-linked hydrogels were made using 0%, 10%, 20% and 30% HPG with respect to PEO. Increasing the HPG content increased the pore size of the hydrogel scaffold, as well as the porosity. The pore size of hydrogel scaffolds could be easily tailored by controlling the content of HPG in the polymer blend. Evaluation of the cytotoxicity demonstrated that HPG/PEO hydrogel can function as a potential material for tissue engineering scaffolds.

This study shows the potential of modified PEO hydrogel films for wound dressing, anti-adhesion barrier and tissue engineering scaffold applications. For future development, combination ionic crosslinking and radiation crosslinking could be an advanced research to produce hydrogel with high mechanical strength and it is necessary to apply the drug loaded hydrogel with traditional medicine to increase the healing effect of hydrogels especially for wound dressing. Variation of molecular weight of PEGDC could be a solution to increase tissue adhesion of hydrogel in anti adhesion barrier application.

REFERENCES

Chapter 1

[1] D. Campoccia, P. Doherty, M. Radice, P. Brun, G. Abatangelo, D.F. Williams, Semi Synthetic Resorbable Materials from Hyaluronan Esterification, Biomaterials 19 (1998) 2101–2127.

[2] G.D. Prestwich, D.M. Marecak, J.F. Marecak, K.P. Ver- cruysse, M.R. Ziebell, Controlled Chemical Modification of Hyaluronic Acid, J. Controlled Release 53 (1998) 93–103.

[3] K. Pal, A.K. Banthia and D.K. Majumdar, Polymeric Hydrogels: Characterization and Biomedical Applications –A mini review, Designed Monomer and Polymers 12 (2009),197-220.

[4] J.M. Rosiak, P. Ulanski, Synthesis of Hydrogels by Irradiation of Polymers in Aqueous Solution, Radiat. Phys. Chem. 55 (1999) 139-151.

[5] F. Yoshi, Y. Zhanshan, K. Isobe, K. Shinozaki, and K. Makuuchi, Electron Beam Crosslinked PEO and PEO/PVA hydrogels for Wound Dressing, Radiat. Phys. Chem. 55 (1999) 133-138.

[6] T.R. Hoare, D.S. Kohane, Hydrogels in Drug Delivery: Progress and challenges, Polymer 49 (2008) 1993–2007.

[7] S.K.H. Gulrez, S. Al-Assaf, G.O. Phillips, Hydrogels: Methods of Preparation, Characterisation and Applications, in: A. Carpi (Eds), Progress in Molecular and Environmental Bioengineering - From Analysis and Modeling to Technology Applications, InTech., United Kingdom, 2011, 117-150.

[8] W.E. Hennink, C.F. van Nostrum, Novel Crosslinking to Design Hydrogel, Adv. Drug Deliv. Rev. 54 (2002) 13-36.

[9] A.S. Hoffman, Hydrogels for Biomedicals Applications, Adv. Drug Deliv. Rev. 54 (2002) 3-12.

[10] J.M. Anderson, J.J. Langone, Issues and Perspectives on the Biocompatibility and Immunotoxicity Evaluation of Implanted Controlled Release Systems, J Control Release. 57 (1999) 107-113.

[11] W.E. Hennink, C.F. van Nostrum, Novel Crosslinking Methods to Design Hydrogels, Adv. Drug Deliv. Rev. 54 (2002) 13-36.

[12] J.M. Rosiak, F. Yoshii, Hydrogels and Their Medical Applications, Nuclear Instruments and Methods in Physics Research Section B, 151 (1999) 56-64.

[13] T. Funami, M. Hiroe, S. Noda, I. Asai, S. Ikeda, K. Nishimari, Influence of molecular structure imaged with atomic force microscopy on the rheological behavior of carrageenan aqueous systems in the presence or absence of cations, Food Hydrocolloids, 21 (2007) 617-629.

[14] A.K. Bajpai, S.K. Shukla, S. Bhanu, S. Kankane, Responive Polymer in Controlled Drug Delivery, Prog in Polym Sci, 33 (2008) 1088-1118.

[15] H. Zhao, X. Zheng, X. Yuan, L. Wang, X. Wang, Y. Zhong, Z. Xie, T. Tully, Ben Functions with Scamp During Synaptic Transmission and Long-term Memory Formation in Drosophila. J. Neurosci. 29 (2009) 414-424.

[16] C. Esteban, D. Severian, Polyionic Hydrogels Based on Xanthan and Chitosan for Stabilizing and Controlled Release of Vitamins. U.S. Patent WO0004086 (A1), January 27, 2000.

[17] M. Takigami, H. Amada, N. Nagasawa, T. Yagi, T. Kasahara, S. Takigami, M. Tamada, Trans. Mater. Res. Soc. Jpn. 32 (2007) 713-716.

[18] P. Giannouli, E.R. Morris, Cryogelation of Xanthan, Food Hydrocolloid, 17 (2003) 495-501.

[19] C. Chang, L. Zhang, J. Zhou, L. Zhang, J.F. Kennedy, Structure and Properties of Hydrogels Prepared from Cellulose in NaOH/urea Aqueous Solutions, Carbohydr. Polym. 82 (2010) 122-127.

[20] S. Spinelli, R. Ramoni, S. Grolli, J. Bonicel, C. Cambillau, M. Tegoni, V. Taglio, The Structure of the Monomeric Porcine Odorant Binding Protein Sheds Light on the Domain Swapping Mechanism, Biochemistry 37 (1998) 7913-7918.

[21] H.M. Said, S.G.A. Alla, A.W.M. El-Naggar, Synthesis and Characterization of Novel Gels Based on Carboxymethyl Cellulose/acrylic Acid Prepared by

Electron Beam Irradiation. Reactive & Functional Polymers 61 (2004) 397-404.

[22] A.B. Lugao, S.N. Malmonge, Use of Radiation in The Production of Hydrogels, Nuclear Instrument and Methods in Physic Research B, 185 (2001) 37-42.

[23] V.S. Ivanov, Radiation Chemistry of Polymers, 1st ed., Koninklijke Wohrmann B.V., The Netherlands.

[24] A. Singh, J. Silverman, eds. Radiation Processing of Polymers. New York, NY: Oxford University Press, 1992.

Chapter 2

[1] J.V. Cartmell, W.R. Sturtevant, M. Valadez, and M.L. Wolf, *Hydrogel wound dressing product*, US Patent 5059424 (1991).

[2] S. Rajendran and S.C. Anand, *Development in Medical Textiles*, The Textile Institute, Manchester, 2002.

[3] L. Jones, C. Maya, L. Nazar, and T. Simpson, *Contact Lens & Anterior Eye*, **25**, 147 (2002).

[4] D.M. Soler, Y. Rodriguez, H.Correa, A. Moreno, L. Carrizales, *Radiat Phys Chem*, **81**, 1249 (2012).

[5] M. George, T.E. Abraham, *Pharmaceutics*, **335**, 123 (2007).

[6] T. Abdelrahman and H. Newton, *Surgery*, **29**, 491 (2011).

[7] Y. Ikada, T. Mita, F. Horii, and I. Sakurada, *Radiat Phys Chem*, **9**, 633 (1977).

[8] S.S. Jang, W.A. Goddard, and M.Y.S. Kalani, *J Phys Chem B*, **111**, 1729 (2007).

[9] J.S. Park, S.J. Gwon, Y.M. Lim, and Y.C. Nho, *Macromol. Res*, **17**, 580 (2009).

[10] F. Yoshi, Y. Zhanshan, K. Isobe, K. Shinozaki, and K. Makuuchi, *Radiat Phys Chem*, **55**, 133 (1999).

[11] X. Zhang, D. Yang, and J. Nie, *Int J Biol Macromol*, **43**, 456 (2008).

[12] C.A. Durst, M.P. Cuchiara, E.G. Mansfield, J.L. West, K.J. Grande-Allen, *Acta Biomater*, **7**, 2467 (2011).

[13] Y.N. Sang, C.N. Young, and H.H. Seung, *Macromol. Res*, **12**, 219 (2004).

[14] K.M. Salmawi and S.M. Ibrohim,*Macromol. Res*, **19**, 1029 (2011).

[15] J.M. Rosiak and P. Ulanski, *Radiat Phys Chem*, **55**, 139 (1999).

[16] A.C. Mesquita, M.N. Mori, and L.G. Andrade e silva, *Radiat Phys Chem*, **71**, 251 (2004).

[17] V.S. Ivanov, *Radiation Chemistry of Polymers*, Koninklijke Wohrmann B.V., Netherlands, 1992.

[18] M. Wu, B. Bao, F. Yoshii, and K. Makuuchi, *J Radioanal Nucl Chem*, **250**, 391(2001).

[19] M.H. Huang and M.C. Yang, *Int J Pharm*, **346**, 38 (2008).

[20] ASTM Standard E96/E96-10, *Standard Test Methods for Water Vapor Transmission of Materials*, ASTM International, West Conshohocken, PA, (2011).

[21] M.T. Razzak, D. Darwis, Zainuddin, and Sukirno, *Radiat Phys Chem*, **62**, 107 (2011).

[22] K. Hirose, H. Onishi, M. Sasatsu, K. Takeshita, K. Kouzuma, K. Isowa, and Y. Machida, *Biological & pharmaceutical bulletin*, **30**, 2406 (2007).

[23] M.R. Hwang, J.O. Kim, J.H. Lee, Y.I. Kim, J.H. Kim, S.W. Chang, S.G. Jin, J.A. Kim, W.S. Lyoo, S.S. Han, S.K. Ku, C.S. Yong, and H.G. Choi, *AAPS Pharm Sci Tech*, **11**, 1092 (2010).

[24] J. Kim, S. Jin, S. Ku, D. Nam, Y. Sohn, D. Ryu, E.S. Do, S. Jang, M. Son, C. Yong, H.G. Choi, and J. Kim, *J Pharm Invest*, **42**, 327 (2012).

[25] J.H. Lee, S.J. Lim, D.H. Oh, S.K. Ku, D.X. Li, C.S. Yong and H.G. Choi, *Arch Pharmacal Res*, **33**, 1083 (2010).

[26] A. Levene, *Clin Otolaryngol Allied Sci*, **6**, 145 (1981).

[27] J. Ludbrook, *Clin Exp Pharmacol Physiol*, **24**, 294 (1997).

[28] J.H. Sung, M.R. Hwang, J.O. Kim, J.H. Lee, Y.I. Kim, J.H. Kim, S.W. Chang, S.G. Jin, J.A Kim, W.S. Lyoo, S.S. Han, S.K. Ku, C.S. Yong, and H.G. Choi, *Int J Pharm*, **392**, 232 (2010).

[29] U.W. Gedde, *Polymer Physics*, Chapman & Hall, London, 1995.

[30] D. Queen, J.D.S. Gaylor, J.H. Evans, J.M. Courtney, W.H. Reid, *Biomaterials*, **8**, 367 (1987).

[31] F.L. Mi, S.S. Shyu, Y.B. Wu, S.T. Lee, J.Y. Shyong, and R.N. Huang, *Biomaterials*, **22**, 165 (2001).

Chapter 3

[1] M.P. Diamond, Incidence of postsurgical adhesion, in: G.S. diZerega, (Eds.), Peritoneal surgery, Springer-Verlag., New York, 2000, pp. 217-220.

[2] T. Liakakos, N. Thomakos, P. M. Fine, C. Dervenis, R. L. Young, Dig. Surg. 18 (2001) 260-273.

[3] H. Ellis, Eur. J. Surg. 577 (1997) 5-9.

[4] R. Marana, M. Rizzi, L. Muzii, Infertility and adhesions in Peritoneal surgery, Springer, New York, 2000, pp. 329–333.

[5] Y. Liu, X.Z. Shu, G.D. Prestwich, Fertil. Steril. 87 (2007) 940-983.

[6] M.W. Lee, H.F. Tsai, S.M. Wen, C.H. Huang, Carbohydr. Polym. 90 (2012) 1132-1138.

[7] A.S. Hoffman, Adv. Drug Deliv. Rev. 54 (2002) 3-12.

[8] W.E. Hennink, C.F. van Nostrum, Adv. Drug Deliv. Rev. 54 (2002) 13-36.

[9] T. Funami, M. Hiroe, S. Noda, I. Asai, S. Ikeda, K. Nishimari, Food Hydrocolloids. 21 (2007) 617-629.

[10] C. Esteban, D. Severian, Polyionic hydrogels based on xanthan and chitosan for stabilizing and controlled release of vitamins. U.S. Patent WO0004086 (A1), January 27, 2000.

[11] M. Takigami, H. Amada, N. Nagasawa, T. Yagi, T. Kasahara, S. Takigami, M. Tamada, Trans. Mater. Res. Soc. Jpn. 32 (2007) 713-716.

[12] R. Barbucci, G. Leone, A. Vecchiullo, J. Biomater. Sci., Polym. Ed. 15 (2004) 607-619.

[13] C. Chang, L. Zhang, J. Zhou, L. Zhang, J.F. Kennedy, Carbohydr. Polym. 82 (2010) 122-127.

[14] H.S. Mansur, C.M. Sadahira, A.N. Souza, A.A.P. Mansur, Mater. Sci. Eng., C 28 (2008) 539-548.

[15] F. Yoshii, T. Kume, Process for producing crosslinked starch derivatives and crosslinked starch derivatives produced by the same. U.S. Patent 6617448, September 9, 2003.

[16] G.Y. Xu, A.M. Chen, S.Y. Liu, S.L.Yuan, X.L. Wei, Acta Phys.-Chim. Sin. 18 (2002) 1043-1047.

[17] R.A. Wach, H. Mitomo, F. Yoshii, T. Kume, J. Appl. Polym. Sci. 81 (2001) 3030-3037.

[18] M. Park, B.S. Kim, H.K. Shin, S.J. Park, H.Y. Kim, Mater. Sci. Eng., C 33 (2013) 5051-5057.

[19] X. Huang, Y. Zhang, X. Zhang, L. Xu, X. Chen, S. Wei, Mater. Sci. Eng., C

33 (2013) 4816-4824.

[20] Y.C. Kuo, Y.R. Hsu, J. Biomed. Mater. Res. 91A (2009) 277-287.

[21] S.J. Bryant, K.S. Anseth, In Photocrosslinkable Poly(ethylene oxide) and Poly(vinyl alcohol) Hydrogels for Tissue Engineering Cartilage, Proceedings of The First Joint BMES/EMBS Conference, Serving Humanity, Advancing Technology, Atlanta, GA, USA, Oct 13-16, 1999; Piscataway: New Jersey ,1999.

[22] P. Brun, F. Ghezzo, M. Roso, R. Danesin, G. Palu, A.A. Bagno, M. Modesti, I. Castagliuolo, M. Dettin, Acta Biomater. 7 (2011) 2526-2532.

[23] J. Kim, K.W. Lee, T.E. Hefferan, B.L. Currier, M.J. Yaszemski, L. Lu, Biomacromolecules 9 (2008) 149-157.

[24] Y.C. Kuo, I.N. Ku, Biomacromolecules 9 (2008) 2662-2669.

[25] A. Lavasanifara, J. Samuela, G.S. Kwonb, Adv. Drug Deliv. Rev. 54 (2002) 169-190.

[26] E.A. Yapar, O. Inal, Trop. J. Pharm. Res. 11 (2012) 855-866.

[27] M.R. Mucalo, M.J. Rathbone, Chemistry in New Zealand 76 (2012) 85-95.

[28] I. Savva, A.D. Odysseos, L. Evaggelou, O. Marinica, E. Vasile, L. Vekas, Y. Sarigiannis, T.K. Christoforou, Biomacromolecules 14 (2013) 4436-4446.

[29] P. Kallinteri, S. Higgins, G.A. Hutcheon, C.B.St. Pourcain, M.C. Garnett, Biomacromolecules 6 (2005) 1885-1894.

[30] Haryanto, S.C. Kim, J.H. Kim, J.O. Kim, S.K. Ku, H. Cho, D.H. Han, P.

Huh, Macromol. Res. 22 (2014) 131-138.

[31] F. Yoshii, Y. Zhanshan, K. Isobe, K. Shinozaki, K. Makuuchi, Radiat. Phys. Chem. 55 (1999) 133-138.

[32] D. O'Sullivan, M. O'Riordain, R.P. O'Connel, M. Dineen, M.P. Brady, Br. J. Surg. 78 (1991) 427-429.

[33] Z. Zhang, J. Ni, L. Chen, J. Xu, J. Ding, Biomaterials 32 (2011) 4725-4736.

[34] V.P. Torchilin, Polymeric Nanomaterials, in: C. S. S. R. Kumar, (Eds.), Nanomaterials for the Life Sciences, Vol. 10, Part 1, WILEY-VCH Verlag GmbH & Co. KGaA., Weinheim, 2011, p 124.

[35] Y. Bai, J. Peng, J. Li, G. Lai, Appl. Organomet. Chem. 25 (2011) 400-405.

[36] B.A. Soltz, D.P. DeVore, B.P. DeVore, R. Soltz, M.A. Soltz, Composite Tissue Adhesive, U.S. Patent 6939364B1, September 6, 2005.

[37] L.S. Liu, R.A. Berg, J. Biomed. Mater. Res. 63 (2002) 326-332.

[38] A. Kumar, S. S. Lahiri, H. Singh, Int. J. Pharm. 323 (2006) 117-124.

[39] J.A. Killion, L.M. Geever, D.M. Devine, J.E. Kennedy, C.L. Higginbotham, J. Mech. Behav. Biomed. Mater. 4 (2011) 1219-1227.

[40] S.K.H. Gulrez, S. Al-Assaf, G.O. Phillips, Hydrogels: Methods of Preparation, Characterisation and Applications, in: A. Carpi (Eds), Progress in Molecular and Environmental Bioengineering - From Analysis and Modeling to Technology Applications, InTech., United Kingdom, 2011, pp 117-150.

[41] X. Dai, Xi. Chen, L. Yang, S. Foster, A.J. Coury, T.H. Jozefiak, Acta Biomater. 7 (2011) 1965–1972.

[42] A.C. Mesquita, M.N. Mori, L.G. Andrade e silva, Radiat. Phys. Chem. 71 (2004) 251-254.

[43] M.M. Khan, S.A. Ansari, D. Pradhan, M.O. Ansari, D.H. Han, J. Lee, M.H. Cho, J. Mater. Chem. A. 2 (2014) 637-644.

[44] T. D. Way, S.R. Hsieh, C.J. Chang, T.W. Hung, C.H. Chiu, Appl. Surf. Sci. 256 (2010) 3330-3336.

[45] M. Wu, B. Bao, F. Yoshii, K. Makuuchi, J. Radioanal. Nucl. Chem. 250 (2001) 391-395.

[46] ASTM Standard D6195-03, Standard Test Methods for Loop Tack, ASTM International, West Conshohocken, 2011.

[47] A. Mishra, N. Chaudhary, Trends Biomater. Artif. Organs. 23 (2010) 122-128.

[48] S. Avital, T.J. Bollinger, J.D. Wilkinson, F. Marchetti, M.D. Hellinger, L.R. Sands, Dis. Colon Rectum. 48 (2005) 153-157.

[49] U.W. Gedde, Polymer Physics, 1st ed., Chapman & Hall, London, 1995.

[50] K.E. Rodgers, H.E. Schwartz, N. Roda, M. Thornton, W. Kobak, G.S. diZerega, Fertil. Steril. 73 (2000) 831-838.

[51] Y. Zhang, C. Gao, X. Li, C. Xu, Y. Zhang, Z. Sun, Y. Liu, J. Gao, Carbohydr. Polym. 101 (2014) 171– 178.

Chapter 4

[1] Yang S, Leong KF, Du Z, Chua CK. The design of scaffolds for use in tissue engineering, part I. traditional factors. Tissue Eng 2001;7:679-689.

[2] Lalwani G, Gopalan A, D'Agati M, Srinivas Sankaran J, Judex S, Qin Y-X, Sitharaman B. Porous three-dimensional carbon nanotube scaffolds for tissue engineering. J Biomed Mater Res Part A 2015;00A:000-000.

[3] Agrawal CM, Ray RB. Biodegradable polymeric scaffolds for musculoskeletal tissue engineering. J Biomed Mater Res 2001;55:141-150.

[4] Boccaccini AR, Maquet V. Bioresorbable and bioactive polymer/bioglass® composites with tailored pore structure for tissue engineering applications. Compos Sci Technol 2003;63: 2417-2429.

[5] Lu L, Mikos AG. The importance of new processing techniques in tissue engineering. MRS Bull 1996;21:28-32.

[6] Chen G, Ushida T, Tateishi T. Scaffold design for tissue engineering. Macromol Biosci. 2002;2:67-77.

[7] Jamalpoor Z, Mirzadeh H, Joghataei MT, Zeini D, Bagheri-Khoulenjani S, Nourani MR. Fabrication of cancellous biomimetic chitosan-based nanocomposite scaffolds applying a combinational method for bone tissue engineering. J Biomed Mater Res Part A 2015;103A:1882-1892.

[8] Hoffman AS. Hydrogels for biomedical applications. Adv Drug Delivery Rev 2002;54:3-12.

[9] Lee KY, Mooney DJ. Hydrogels for tissue engineering. Chem Rev 2001;101:1869-1879.

[10] Hennink WE, van Nostrum CF. Novel crosslinking methods to design hydrogels. Adv Drug Deliv Rev 2002;54:13-36.

[11] Mansur HS, Sadahira CM, Souza AN, Mansur AAP. FTIR spectroscopy characterization of poly(vinyl alcohol) hydrogel with different hydrolysis degree and chemically crosslinked with glutaraldehyde. Mater Sci Eng C 2008;28:539-548.

[12] Wach RA, Mitomo H, Yoshii F, Kume T. Hydrogel of biodegradable cellulose derivatives. II. effect of some factors on radiation-induced crosslinking of cmc. J Appl Polym Sci 2001;81:3030-3037.

[13] Park M, Kim BS, Shin HK, Park SJ, Kim HY. Preparation and characterization of keratin-based biocomposite hydrogels prepared by electron beam irradiation. Mater Sci Eng C 2013;33:5051-5057.

[14] Temenoff JS, Mikos AG. Injectable biodegradable materials for orthopedic tissue engineering. Biomaterials 2002;21:2405-2412.

[15] Elisseeff J, Anseth K, Sims D, McIntosh W, Randolph M, Langer R. Transdermal photopolymerization for minimally invasive implantation. Proc Natl Acad Sci 1999;96: 3104-3107.

[16] Hahn MS, McHale MK, Wang E, Schmedlen RH, West JL. Physiologic pulsatile flow bioreactor conditioning of poly(ethylene glycol)-based tissue

engineered vascular grafts. Ann Biomed Eng 2007;35:190-200.

[17] Kuo YC, Hsu YR. Tissue-engineered polyethylene oxide/chitosan scaffolds as potential substitutes for articular cartilage. J Biomed Mater Res 2009;91:277-287.

[18] Brun P, Ghezzo F, Roso M, Danesin R, Palu G, Bagno AA, Modesti M, Castagliuolo I, Dettin M. Electrospun scaffolds of self-assembling peptides with poly(ethylene oxide) for bone tissue engineering. Acta Biomater 2011;7:2526-2532.

[19] Kim J, Lee KW, Hefferan TE, Currier BL, Yaszemski MJ, Lu L. Synthesis and evaluation of novel biodegradable hydrogels based on poly(ethylene glycol) and SE-beamacic acid as tissue engineering scaffolds. Biomacromolecules 2008;9:149-157.

[20] Lavasanifara A, Samuela J, Kwon GS. Poly(ethylene oxide)-block-poly(L-amino acid) micelles for drug delivery. Adv Drug Deliv Rev 2002;54:169-190.

[21] Yapar EA, Inal O. Poly(ethylene oxide)–poly(propylene oxide)-based copolymers for transdermal drug delivery: An overview. Trop J Pharm Res 2012;11:855-866.

[22] Mucalo MR, Rathbone MJ. Melt-extruded polyethylene oxide (PEO) rods as drug delivery vehicles: Formulation, performance as controlled release devices and the influence of co-extruded excipients on drug release profiles.

Chem N. Z 2012;76:85-95.

[23] Haryanto, Kim SC, Kim JH, Kim JO, Ku SK, Cho H, Han DH, Huh P. Fabrication of poly(ethylene oxide) hydrogels for wound dressing application using e-beam. Macromol Res 2014;22:131-138.

[24] Haryanto, Deepti S, Han SS, Son JH, Kim SC. Poly(ethylene glycol) dicarboxylate/poly(ethylene oxide) hydrogel film co-crosslinked by electron beam irradiation as an anti-adhesion barrier. Mater Sci Eng C 2015;46:195-201.

[25] O'Sullivan D, O'Riordain M, O'Connel RP, Dineen M, Brady MP. Peritoneal adhesion formation after lysis: Inhibition by polyethylene glycol 4000. Br J Surg 1991;78:427-429.

[26] West JL, Hubbell JA. Polymeric biomaterials with degradation sites for proteases involved in cell migration. Macromolecules 1999;32:241-244.

[27] Mann BK, Gobin AS, Tsai AT, Schmedlen RH, West JL. Smooth muscle growth in photopolymerized hydrogels with cell adhesive and proteolytically degradable domains: Synthetic ECM analogs for tissue engineering. Biomaterials 2001;22:3045-3051.

[28] Bryant SJ, Anseth KS. The Effects of scaffold thickness on tissue engineered cartilage in photocrosslinked poly(ethylene oxide) hydrogels. Biomaterials 2001;22:619-626.

[29] Lee JH, Lee HB, Andrade JD. Blood compatibility of polyethylene oxide

surfaces. Prog Polym Sci 1995;20:1043-1079.

[30] Nuttelman CR, Tripodi MC, Anseth KS. Synthetic hydrogel niches that promote hMSC viability. Matrix Biol 2005;24:208-218.

[31] Nuttelman CR, Rice MA, Rydholm AE, Salinas CN, Shah DN, Anseth KS. Macromolecular monomers for the synthesis of hydrogel niches and their application in cell encapsulation and tissue engineering. Prog Polym Sci 2008;33:167-170.

[32] Lutolf MP, Hubbell JA. Synthetic biomaterials as instructive extracellular micro environments for morphogenesis in tissue engineering. Nat Biotechnol 2005;23:47-55.

[33] Tibbitt MW, Anseth KS. Hydrogels as extracellular matrix mimics for 3D cell culture. Biotechnol Bioeng 2009;103:655-663.

[34] Kainthan RK, Janzen J, Levin E, Devin DV, Brooks DE. Biocompatibility testing of brench and linear polyglycidol. Biomacromolecules 2006;7:703-709.

[35] Yoshii F, Zhanshan Y, Isobe K, Shinozaki K, Makuuchi K. Electron beam crosslinked PEO and PEO/PVA hydrogels for wound dressing. Radiat Phys Chem 1999;55:133-138.

[36] Khan MM, Ansari SA, Pradhan D, Han DH, Lee J, Cho MH. Defect-induced band gap narrowed CeO2 nanostructures for visible light activities. Ind Eng Chem Res 2014;53: 9754-9763.

[37] Mesquita, AC, Mori MN, Andrade e silva LG. Polymerization of vinyl acetate in bulk and emulsion by gamma irradiation. Radiat Phys Chem 2004;71:253-256.

[38] Xia Z, Patchan M, Maranchi J, Elisseeff J, Trexler M. Determination of crosslinking density of hydrogels prepared from microcrystalline cellulose. J Appl Polym Sci 2013;127:4537-4541.

[39] Liu Y, Ma L, Gao C. Facile fabrication of the glutaraldehyde cross-linked collagen/chitosan porous scaffold for skin tissue engineering. Mater Sci Eng C 2012;32:2361-2366.

[40] Pereira AGB, Paulino AT, Rubira AF, Muniz EC. Polymer-polymer miscibility in PEO/cationic starch and PEO/hydrophobic starch blends. eXPRESS Polym Lett 2010;4: 488-499.

[41] Yang S, Leong KF, Du Z, Chua CK. The design of scaffolds for use in tissue engineering-part I: Traditional factors. Tissue Eng 2001;7:679-689.

[42] Li J, Pan J, Zhang L. Culture of hepatocytes on frutose-modified chitosan scaffolds. Biomaterials 2003;24:2317-2322.

[43] Ma L, Gao C, Zhou J, Shen J, Hu X, Han C. Collagen/chitosan porous scaffolds with improved biostability for skin tissue engineering. Biomaterials 2003;24:4833-4841.

[44] Gong YH, Zhou QL, Gao CY, Shen JC. In Vitro and in vivo degradability and cytocompatibility of Poly(L-lactic acid) scaffold fabricated by a gelatin

particle leaching method. Acta Biomater 2007;3:531-540.

[45] Hao Y, Peng J, Li J, Zhai M, Wei G. An ionic liquid as reaction media for radiation-induced grafting of thermosensitive poly(N-isopropylacrylamide) onto microcrystalline cellulose. Carbohydr Polym 2009;77:779-784.

전자빔을 이용한 개질된 폴리에틸렌옥사이드 하이드로겔 필름의 제조와 의학적 응용

하리안토

영남대학요 대학원

유기신소재공학과 – 유기신소재공학전공

지도교수: 김성철

요약

최근들어 합성고분자를 이용한 하이드로겔은 생체적합성, 수분흡수성, 생분해성과 적절한 기계적 강도로 인해 바이오 및 의료용 소재로써 천연고분자 하이드로겔보다 더 많은 주목을 받고 있다. 따라서 본 연구는 폴리에틸렌옥사이드(PEO)를 기반으로 폴리에틸렌 글리콜 디아크릴레이트(PEGDA), 폴리에틸렌 글리콜디카르복실레이트(PEGDC), 폴리에틸렌글리콜 디메타크릴레이트, 하이퍼브랜치 폴리글리시돌 등의 물질을 폴리에틸렌옥사이드에 소량 첨가하여 전자빔을 이용해 가교한 후 창상피복제, 유착방지막, 조직공학용 지지체 등에 적용하였다.

전자빔을 이용해 가교된 PEGDA/PEO 하이드로겔을 이용해 창상피복제를 제조하였는데, PEO의 분자량을 달리하고, 조성과 방사선량을 조절해 가교 밀도를 조절하였다. PEGDA의 양은 겔과도, 팽윤도, 기계적강도와 수분투과도 등에 영향을 미침을 확인하였다. 하이드로겔 드레싱을 이용한 상처치유 과정은 실험용 쥐를 이용해서 상업적으로 판매되는 제품 및 거즈만 사용한 대조군과 비교실험을 진행하였다. 그 결과 상업적으로 판매되는 제품과 비교해서 치유특성이 손색이 없고, 대량생산이 가능하고 기계적 강도가 뛰어나며 투명한 창상피복제를 만들 수 있었다.

가교된 PEGDC/PEO와 PEGDMA/PEO를 이용해 유착방지필름을 제조하였다. 3개의 다른 조성(10% PEGDC, 10% PEGDMA, 5% PEGDC-5% PEGDMA) 을 이용해 가교 하이드로겔 필름을 제조하였고, 이 재료들 중에서 10% PEGDC 하이드로겔 필름이 가장 좋은 조직점착성을 보여주었다. 이 결과는 카르복시기가 조직의 점막과 같은 곳에 수소결합 등으로 잘 점착될 수 있음을 보여준다. 동물 실험을 통해 10% PEGDC 하이드로겔 필름이 시판되는 국산 제품인 Guardix-SG®보다도 더 뛰어난 유착방지특성을 보임을 확인하였다.

앞서의 실험과 동일한 방법으로 HPG와 PEO를 이용해 마이크로기공의 하이드로겔 지지체가 제작되었다. 이 실험에서 trimethylol propane을 core로 사용하고 글리시돌을 단량체로 사용해 HPG를 음이온 중합법으로 합성하였고, PEO에 대해 각각 0%, 10%, 20% 및 30%씩 혼합하여 전자빔을 이용해 가교하였다. HPG의 함량이 증가할수록 하이드로겔 지지체의 기공 크기가 기공도와 함께 증가하는 것을 확인할 수 있었다. 이는 HPG의 함량을 조절하여 기공도와 기공크기를 조절할 수 있음을 의미한다. 세포독성의 평가를 통해 HPG/PEO 하이드로겔이 조직공학용 지지체로 사용이 적합함을 알 수 있었다.

이와 같은 일련의 실험으로 PEO를 적절한 가교제와 첨가물의 양을 조절하여 가교된 하이드로겔 필름을 쉽게 제조할 수 있었고, 이를 이용해서 창상피복제, 유착방지막 및 조직공학용 지지체로 효과적으로 이용할 수 있었다.

LIST OF PUBLICATIONS

[1] Haryanto, Kim SC, Kim JH, Kim JO, Ku SK, Cho H, Han DH, Huh P. Fabrication of poly(ethylene oxide) hydrogels for wound dressing application using e-beam. Macromol Res 2014;22:131-138.

[2] Haryanto, Deepti S, Han SS, Son JH, Kim SC. Poly(ethylene glycol) dicarboxylate/poly(ethylene oxide) hydrogel film co-crosslinked by electron beam irradiation as an anti-adhesion barrier. Mater Sci Eng C 2015;46:195-201.

[3] Haryanto, Deepti S, Huh P, Kim SC. Hyperbranched poly(glycidol) / poly(ethylene oxide) hydrogels cross-linked by e-beams as microporous scaffolds for tissue engineering applications. Biomedical Materials research part A 2015 (Accepted, June 2015).

[4] Kim Seong Cheol, Haryanto, Son Jun Hyeok, Method for manufacturing biodegradable polymer film and biodegradable polymer for anti-adhesion, Korea Patent, 1013656150000, February, 14, 2014.